INVESTIGATION INTO MAMMALIAN OS CORDIS AND CARTILAGO CORDIS

Masters of Research Thesis

Adam Best

Dr. Catrin Rutland, Dr. Craig Sturrock, Dr. Nigel Mongan, Dr. Kerstin Baiker

University of Nottingham [Student Number: 4295843]

The University of Nottingham

UNITED KINGDOM · CHINA · MALAYSIA

School of **Veterinary Medicine and Science**

Page of Contents

List of Figures

List of Tables

Abbreviations

ALPL……………………………………………………Alkaline Phosphatase

AVN…………………………………………………Atrioventricular Node

CVD…………………………………………………Cardiovascular Disease

EO…………………………………………………Endochondral Ossification

G3…………………………………………………Gorilla Heart Number 3

G11…………………………………………………Gorilla Heart Number 11

HO…………………………………………………Heterotopic Ossification

H+E…………………………………………………Hematoxylin and Eosin

IMF…………………………………………Idiopathic Myocardial Fibrosis

IMO…………………………………………Intramembranous Ossification

MicroCT…………………………………………Computed Microtomography

OCD…………………………………………………Os Cordis Dextrum

OCS…………………………………………………Os Cordis Sinistrum

ROI…………………………………………………Regions Of Interest

Acknowledgments

Graphical Abstract

A Comprehensive Look at Os Cordis and Cartilgo Cordis Including the Investigation of Four Mammals

2 Anatomical investigation of the hearts of 4 mammals

Nyala n=1

Giraffe n=1

Gorilla n=15

Bonobo n=9

1 Comprehensive review of all previously investigated species

3 By collecting data from the review and our own investigations we could identify genetic trends regarding the presense, formation and function of os cordis and cartilago cordis

Dissesction   MicroCT   Microscopy   Presence or lack of os/cartilago cordis in the heart

Abstract

This thesis includes a comprehensive literature review of the two major hyperdense tissue types found in the heart: bone and cartilage known as os cordis and cartilago cordis respectively. Alongside this review is an investigation of the cardiac tissue in four mammalian species. The nyala, giraffe, Gorilla and bonobo were all examined using computed microtomography (microCT) and histological techniques. The study included an investigation of 26 hearts across the four mammalian species (nyala n= 1; giraffe n= 1; Gorilla n= 15; bonobo n= 9). The review showed that 13 species had been found with os cordis and 24 species had cartilago cordis present. Having collated all data from these investigations it was possible to observe that os cordis development can occur as a normal anatomical event or, in other species, may form as a direct result of cardiovascular disease. Additionally, how the cartilago cordis forms is yet to fully understood, although is likely to involve neural crest cells. In addition, the formation of os cordis is likely to occur by endochondral ossification (EO) from cartilage, which may more may not, be related to cartilago cordis. Suggested functions of os cordis and cartilago cordis appear to be similar, as a protective structure in areas of high mechanical stress or to aid in contraction. Our own investigations into the nyala, giraffe, Gorilla and bonobo involved X-ray computed microtomography, dissection and histology. The nyala was found to have four ossa cordis, a novel discovery, while the giraffe had one single os cordis. No bone or cartilage were found in the Gorilla or bonobo. Both nyala and giraffe bones showed direct evidence of EO and the presence of os(sa) cordis in both of these species confirmed suggestions that os(sa) cordis occurrence may be linked to genetics since nyala, giraffe and many species with os cordis found in the review originated from the *Artiodactyla* order. Although neither bone nor cartilage was found in the Gorilla or bonobo hearts, the investigation allowed us to assess fibrosis levels within each heart, a factor which has been shown to directly correlate with os cordis formation.

1. Introduction

The purpose of this study was to enhance the understanding of hyperdense tissues within the heart notably, os and cartilago cordis. In addition to greater anatomical knowledge, a better understanding of these structures may prompt further studies to investigate how these structures effect the tissues around them, particularly in association with CVD.

1.1. Cardiac Anatomy

All mammalian hearts have a similar structure and function. Each side of the heart has two types of major chambers, an atrium which feeds blood into a ventricle which then contracts that blood out of the heart. Stages of contraction are known as systole while phases of relaxation are known as diastole. In adults, the right and left sides of the heart are divided by interatrial and interventricular septa between the atria and ventricles respectively (Singha, 2018). On the right side of the heart blood is forced out through the pulmonary artery to the lungs, and on the left side of the heart blood is forced out via the aorta to the rest of the body. The four chambers are surrounded by internal supporting fibrous tissue (cardiac skeleton) and muscular tissue (myocardium;

Anderson et al. 2009). Muscular contraction is controlled by the atrioventricular node (AVN) which sends periodic impulses of electricity through the heart via conductive fibers. In order to ensure efficient delivery of electrical impulses, a major collection of conductive fibers, the bundle of His, travels through the interventricular septum to the apex of the heart (Sjaastad et al. 2010).

1.1.1. The Cardiac Skeleton

The cardiac skeleton is a fibrous structure made up of collagen and elastin fibers which act to maintain the hearts shape during systole (Ghonimi et al. 2014). The cardiac skeleton is made up of two trigones, left and right-sided, each incorporating an atrioventricular ring (Figure. 1.1; Ghonimi et al. 2014). The trigones can contain fibrocartilage, hyaline cartilage and, on occasion, bone (Gopalakrishnan et al. 2007). Bone (or bones), when present, are known as os(sa) cordis (Singha, 2018). Cartilage can also be found in the cardiac skeleton and when present as a distinct structure within the trigone region, is referred to as the cartilago cordis. In some species, including humans, an additional thickening at the base of the aorta occurs, known as the cardiac fulcrum. This structure is thought to anchor cardiac muscle to improve the power and efficiency of contractions (Figure. 1.1; Trainini et al. 2020).
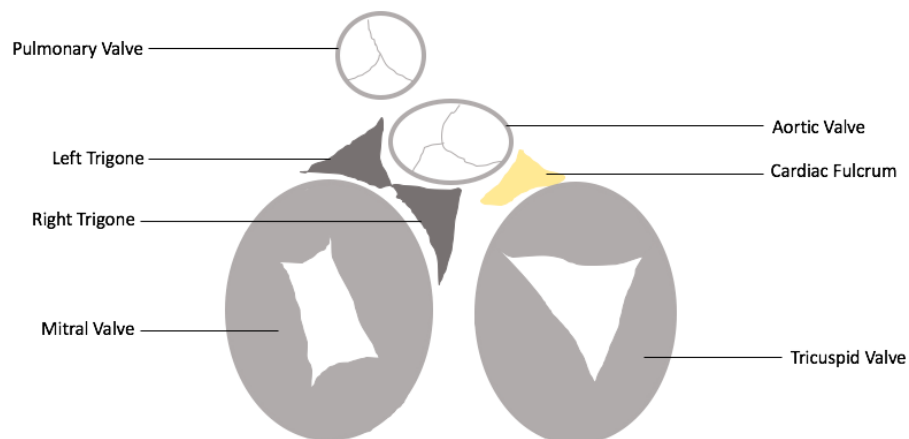
Figure. 1.1. A representation of the relative position of trigones and the fulcrum in the mammalian heart. Adapted from (Hansen & Lambert, 2005).

1.2. Cardiovascular Disease

Cardiovascular disease (CVD) can occur as a result of many different pathological processes. However, many CVDs often have an impact on the conditions affecting the heart. Some of these conditions may have a direct impact on cardiac physiology, such as ischemia and tissue repair (Lehoczky-mona & McCandles, 1964; Aljinovic et al. 2016).

1.2.1. Myocardial Fibrosis

Myocardial fibrosis is a CVD which causes collagen fibers to replace cardiac muscle and is caused by external stimuli such as volume overload or increased cardiac pressure (Lammey et al. 2008). The disease can occur in many species including humans and primates and in some cases can cause arrhythmias resulting in sudden death (Lowenstine et al. 2016). Myocardial fibrosis can be especially prevalent in captive species, particularly primates. A study of chimpanzees found that 91% of 33 captive chimpanzees presented with myocardial fibrosis compared to none of 25 sanctuary housed chimpanzees (Strong et al. 2020).

1.2.2. Cardiac Plaque

Dystrophic calcification is the deposition of calcium within soft tissues as part of a necrotic response to injury (Shackley et al. 2011). Dystrophic calcification in the heart has been observed in mammalian species such as hamsters and is often attributed to CVD (Bajusz, 1969). In separate processes, other plaques which can form as a result of a chronic inflammatory condition. For example, atherosclerosis occurs when plaques, comprised of fat and immune cells, form within vasculature (Falk, 2006).

1.3. Histology

This thesis explores the structure and function of the heart via a number of methods including histological techniques. Histology enables the clear identification of cells and tissues within a sample using stains and observation through a microscope (Ross & Pawlina, 2016). General stains such as haematoxylin and eosin (H+E) can be used to observe tissue morphology and identify cells types. Special stains can also be used to specifically target and identify tissues or cell types. This study used a variety of special stains including von Kossa stain to identify calcium deposits in plaques and bone (Meloan & Puchtler, 1985). Picrosirius red (PSR) staining was used to identify varying collagen types in heart tissues (Lattouf et al. 2014). Alcian blue positively identifies acidic polysaccharides, such as glycosaminoglycan present in cartilage (Kumar & Kiernan, 2010). Finally, immunohistochemistry, involves exposing the tissue to a specific target antibody to detect for specific cell types. The chosen antibody was for alkaline phosphatase (ALPL), selected to specifically highlight osteoblasts present in bone tissue (Aguiar et al. 2011, Gade et al. 2011).

1.3.1. Histology of Heart Tissues

The cardiac wall consists of three layers: the outer pericardium, the inner endocardium and a layer of thick myocardium in between (Sjaastad et al, 2016). Muscle fibers within the myocardium are made up of cardiomyocytes which can present with multiple nuclei (Ross & Pawlina, 2016). To ensure cardiac muscle acts efficiently pacemaker cells are apparent. Most commonly these are present in atrial nodes where they elicit action potentials producing muscular contraction (Yaniv et al. 2015). Other cells types observed within the heart include adipocytes, often found within connective tissue, and

erythrocytes, found within capillaries. An abundance of erythrocytes or adipocytes within myocardium can be indicative of CVD (Ross & Pawlina, 2016). Erythrocytes are also present within coronary blood vessels composed of layers of thin endothelial cells and smooth muscle. Fibroblasts can be identified within the connective tissues in the heart alongside cells of the immune system such as mast cells (Tirziu et al. 2010).

1.3.2. General Histology of Cardiac Hyperdense Tissues

Hyperdense tissues found in the heart consist of bone, cartilage or dystrophic calcification (plaque). Cartilage itself contains no vasculature or nervous tissue and is made up of chondrocytes within a ground substance of mainly collagen (Sjaastad, 2016). Dystrophic calcification contains no cell types but instead is an accumulation of chemical compounds such as calcium phosphate (Wu et al. 2020). Bone, when fully developed contains inner trabecular (spongy) bone and outer cortical (compact) bone all surrounded by periosteum (Sjaastad, 2016). Bone tissue can display three different cells types (osteocytes, osteoblasts and osteoclasts). Unlike cartilage, bone does contain blood vessels, again composed of layers of thin endothelial cells and smooth muscle (Ross & Pawlina, 2016).

1.4. Ossification

Ossification is the formation of bone and occurs primarily through two processes, endochondral ossification (EO) and intramembranous ossification (IMO). EO occurs via the calcification of cartilage which, in turn, usually develops into cancellous bone and eventually mature bone (Ghonimi et al. 2014). IMO occurs when mesenchymal cells differentiate into osteoblasts which then produce bone tissue directly (Berendsen & Olsen, 2015). Both of these processes are naturally occurring during skeletal development, bone remodeling and repair. However, bone formation can occur within soft tissues, which is known as heterotopic ossification (HO) and is often related to pathology. HO can occur via EO, IMO or a combination of both, and is frequently triggered by systemic changes (Meyers et al. 2019).

1.5. X-ray Computed Microtomography (microCT)

Computed tomography has been used as an imaging technique to produce three-dimensional images from two dimensional X-ray projections. MicroCT uses the same technique but focused on smaller specimens. Since its development in the 1980's microCT has been used to detect hyperdense tissues including bone. Most recently, the technique was used to detect os cordis within the chimpanzee heart (Moittie et al. 2020).

1.6. Dissertation Overview and Rationale

The first results chapter of this thesis, Chapter 3, provides a detailed literature review into os cordis and cartilago cordis, and therefore contains more detailed information into each of these structures. By systematically collecting all previously published information pertaining to the os cordis and cartilago cordis, it was possible to generate a deeper level of understanding surrounding the physiology of these structures including their presentation (Section 3.2 + 3.7), formation (Section 3.3 + 3.8) and function (Section 3.4 + 3.9) as well as their impact on cardiovascular health (Section 3.5).

Chapter 4 of this thesis focusses around investigating hearts from a nyala and giraffe. Investigating hyperdense tissues in the nyala and giraffe pertaining to the discovery of os(sa) cordis in both of these species will enhance anatomical cardiovascular knowledge. As well as this, by studying the phylogeny of the nyala and giraffe, trends may be identified which could suggest similar discoveries, regarding hyperdense tissues, may be found in other species with a similar phylogeny, which are yet to be fully investigated.

The final major investigation included in this study was the investigation of 24 hearts from Gorillas and bonobos (Chapter 5). By analysing two great ape species, the aims were to analyse these species not previously investigated and develop greater clarity surrounding the links between idiopathic myocardial fibrosis (IMF) in apes and the presence of hyperdense structures, as previously seen in the chimp (Moittie et al. 2020). In addition, an investigation into hyperdense tissues in hearts, which may or may not be impacted by disease, could provide more information on the pathogenesis of some CVDs affecting heart tissue, with particular reference to the formation of hyperdense tissues.

1.6.1. Aims, Objectives and Hypothesis

The investigations included in this thesis looked to identify the major hypotheses suggested in previous literature regarding the formation and function of hyperdense structures. These mechanisms of formation could then be investigated via naturally occurring os cordis versus development of hyperdense tissue with influence from CVD. In addition, the work aimed to provide further information about os cordis in general by looking at new species of interest and by imaging ossa cordis using new methods. To achieve these aims and test these hypotheses, all previously published investigations into cardiovascular hyperdense tissues were reviewed and compared to gain phylogenetic data to identify trends between species and to understand ossa cordis structure, function and development. The hearts from two species which aligned with the phylogenetic data but had not been reported to have ossa cordis were investigated, the nyala and giraffe. Additionally, the hearts from two species with a greater likelihood for CVD influence, the Gorilla and bonobo were also investigated. The overarching aims of this thesis were to investigate the structure, function and development of ossa cordis, and investigate potential factors affecting its existence in all species.

Prior to reviewing previously published studies, it was hypothesised that EO contributed towards the formation of os(sa) cordis, as has been observed in other species (Daghash & Farghali, 2017; Ergerbacher et al. 2000; Ghonimi et al. 2014; Moittie et al. 2020; Gopalakrishnan, 2007). It was also hypothesised that the function of that bone would be related to the protection of heart tissues as well as possible involvement to aid myocardial contraction. It was also hypothesised that hyperdense tissues could form as a result of CVD processes, which should be considered separately from the natural development of hyperdense tissues as the heart develops with age/growth.

There were no previously published research articles stating that the nyala, Gorilla or bonobo have hyperdense cardiac tissue/os cordis. There was one published article stating that a giraffe had an os cordis but this was one sentence in a paper and no further work was elaborated upon and no proof was provided that this was bone tissue (Perez et al. 2008). The overarching hypothesis for the investigation of the nyala and giraffe heart was that cardiac hyperdense tissues would be detectable by microCT, and that these tissues would be either cartilage or bone.

The hypotheses regarding the investigation of Gorilla and bonobo hearts were that hyperdense tissues may be discovered, as they were species closely related to the chimpanzee where os cordis was present. If found, it was hypothesised that they would be positively associated with levels of fibrosis within the heart.

2. Materials and Methods
All research included in this thesis received ethical approval from the University of Nottingham School of Veterinary Medicine and Science ethics committee under UK approved ethical guidelines (ethics number: 3186200604). None of the animals involved in this study died for the purposes of research. Following death, 15 Gorillas, nine bonobos, a giraffe and a nyala underwent post mortem by the Laboratory Dedicated to Zoo, Exotic and Wildlife Pathology and were subsequently received by the University of Nottingham and fixed in 10% neutral buffered formalin.

2.1. Literature Review
The literature review included in this thesis considered the presentation, formation and function of os cordis and cartilago cordis. Keyword searches (Table. 2.1) were implemented across three databases (Nusearch, CAB abstracts and pubmed.gov) as well as a further search using google scholar. A total of 33 relevant papers were collected and evaluated within the review (Appendix. 2).

Os cordis
Os cordis AND heart anatomy
Os cordis AND histology
Os cordis AND cardiac anatomy
Osteocyte AND heart
Osteocyte AND cardiac skeleton
Osteocyte AND myocardium AND cardiac skeleton
Osteoblast AND heart
Osteoblast AND heart AND cardiac skeleton
Fulcrum AND osteocyte
Fulcrum AND heart
Fulcrum AND osteocyte AND heart

Table. 2.1. All the keyword searches used to obtain all relevant papers which were used in the literature review of this thesis.

2.2. MicroCT

With the exception of the giraffe heart, where a sample of heart tissue was scanned after dissection, all hearts were first analysed using microCT to detect any hyperdense tissues. Each heart and the single giraffe heart sample (obtained through dissection, see Section 2.3) were wrapped in sheets of X-ray transparent polyethylene and secured in plastic sample containers. Using a cone beam X-ray microCT scanner each heart/ sample was scanned at 120 kV and 200 µA to optimise detection of hyperdense tissues. The microCT scanner used a detector exposure time of 250-333ms, accounting to a total scanning time of 40-45 minutes and taking many projection images through a full 360º rotation. Image data from the microCT was visualised using VGStudioMAX v2.2Software (Volume Graphics GmbH, Heidelberg, Germany). Additionally, datos|x software's inline median smoothing filters were used to produce a 3D reconstruction of the scanning data (GE Sensing and Inspection Technologies GmbH, Wunstorf, Germany).

2.3. Dissection Prior to Tissue Processing and Embedding

Prior to microCT scanning, the giraffe heart was washed using tap water and left to dry fully before investigative dissection in a downward flow chamber (Rutland lab, Univeristy of Nottingham). Working from apex to base, sections of the heart were resected and palpated for hyperdense tissues. One of these sections, found in the region of the interatrial septum, felt more dense on palpation, indicative of hyperdense tissue and so this region was excised from the section and scanned using microCT (see Section 2.2). Five samples were taken from the region with suspected hyperdense tissue found in the giraffe (labelled A-E) as well as one sample of myocardial tissue close to the same region.

Seven samples were harvested from the nyala heart (labelled 1-7). One sample was taken from the right atrial wall (5), two samples were taken from the base of the aorta (6+7), two samples were taken from the regions of the major cardiac septa (1+2) and two samples were taken from myocardial tissue within the wall of the heart (3+4; Figure. 4.2). Between one and five samples were taken from each of the great ape hearts depending on the number of hyperdense regions identified during microCT scanning. These samples were taken from various locations including the base of the aorta, atrioventricular valves, atrial wall, interatrial septum, interventricular septum and aortic tissue.

Regarding the Gorilla, bonobo and nyala heart(s), any regions of interest (ROI; labelled x-z) identified by detection of hyperdense tissues in the microCT scan were transected. Additionally, with the Gorilla and bonobo hearts, representative samples of each ROI were taken from similar regions in other hearts of varying ages and fibrosis levels (labelled A-C). A total of 20 ROI's were identified and a total of 69 samples were taken from the ROI's and representative samples.

2.4. Processing of Heart Samples

Processing of each sample occurred prior to staining as follows (Rutland lad, Univeristy of Nottingham). Each tissue sample from all four species was dehydrated in a series of ethanol solutions (VWR International Limited, USA) for at two hours each (50, 70, 90 and 100%) followed by xylene (VWR International Limited, USA) for two hours. All samples were immersed in paraffin wax for 24 hours before being heated to $60^{o}C$ in an oven for four hours and mounted in a mold and cassette with fresh molten paraffin wax. The sample blocks were sectioned by Aziza Alibhai and the author of this dissertation at a thickness of 7µm using a microtome and N35 blade. For each sample, 60-300 serial sections of tissue were mounted onto 20-100 polysilinated microscope slides (Fisher Scientific, UK). Slides were dried on a $50^{o}C$ heat plate then dried at room temperature dried 24 hours prior to staining.

2.5. Hematoxylin and Eosin Staining Protocol

Hematoxylin and Eosin (H+E) stain was performed on to give a good histological view of all samples and was used extensively within this thesis. Sections were processed by deparaffinisation in xylene (VWR International Limited, USA) for five minutes then rehydration in graded ethanol's (VWR International Limited, USA) for five minutes each (100, 90, 70%) followed by deionised water (dH$_2$O) for five minutes. After processing, sections were incubated in hematoxylin (Merck Life Sciences, UK) for three minutes, washed in tap water for three minutes then incubated in industrial methylated spirit (IMS) solution (VWR International Limited, USA) for 15 seconds. Sections were then washed in tap water again for three minutes, incubated in 1% ammoniated water for 15 seconds and washed once more, in tap water for three minutes. Sections were incubated in eosin (Merck Life Sciences, UK) for five minutes followed by a final three-minute wash in tap water. Sections were dehydrated in dH$_2$O then graded ethanol (70, 90, 100%; VWR International Limited, USA) for five minutes each. Coverslips (Scientific Laboratory Supplies Limited, UK) were adhered to the slides (VWR International Limited, USA) using DPX mounting media (Merck Life Sciences, UK).

2.6. Picrosirius Red Staining Protocol

PSR stain was performed to identify different collagen types within samples (Lattouf et al. 2014). Sections were processed using the same method outlined in Section 2.5. Tissue sections were then incubated for one hour with picrosirius red stain (ab150681, Abcam, UK) in a humidifying chamber. Excess stain was tapped off each slide and sections were washed twice with acetic acid then once with 100% ethanol before being submerged in 100% ethanol (VWR International Limited, USA) for 10 minutes. Coverslips (Scientific Laboratory Supplies Limited, UK) were adhered to the sections using DPX mounting media (Merck Life Sciences, UK).

2.7. Immunohistochemistry Staining Protocol

Immunohistochemistry was performed using ALPL antibody to specifically identify osteoblasts, which contain the ALPL enzyme (Rutland et al. 2021). The stain was performed using an immunohistochemistry kit containing Peroxidase block, Protein block, Post primary antibody, Novolink polymer and diaminobenzidine stain (DAB; 7150-K, Leica Biosystems, Germany). Sections were either exposed to the chosen antibody (1:100 ALPL, PA5-21332, Thermo Fisher, UK) or were selected as negative controls which received no primary antibody. The ALPL antibody was chosen following sequence alignment results undertaken using BLAST software (NCBI, USA). Sections were deparrafinised and rehydrated using the methods outlined in Section 2.5, then antigen retrieval was undertaken by heating the sections in 1mM sodium citrate in a microwave on medium power for 20 minutes. After cooling for a further 20 minutes, slides were placed into dH$_2$O for 5 minutes then placed in a humidifying chamber. Peroxidase block was added to each slide to remove activity of endogenous peroxidase and was incubated for 5 minutes, washed twice with phosphate buffered solution (PBS; Fisher Scientific, UK) and left for 5 minutes after each wash. Protein block was then

added to each slide, acting to reduce non-specific binding, and was incubated for 30 minutes before being washed twice with PBS and left for 5 minutes after each wash. 20ul of primary antibody solution (1 part ALPL to 100 parts 5% fetal calf serum) was added to each slide, incubated for one hour then washed twice with PBS (Fisher Scientific, UK) and left for 5 minutes after each wash. Post primary antibody was added to detect the primary antibody and was added to each slide and incubated for 30 minutes. Then, the same procedure was utilised for the Novolink polymer solution which recognises post primary and any tissue-bound antibodies. After each incubation the slides were washed twice with PBS (Fisher Scientific, UK) and left for 5 minutes after each wash. Finally, 5% DAB was added to the slides which, if the target antibody was present, produced a visible brown precipitate at the antigen site. DAB was left for 10-20 seconds until the stain had been taken up by the sections. At this point, sections were immediately counterstained in hematoxylin for three seconds. Sections were then dehydrated and coverslipped using the methods outlined in Section 2.5.

2.8. Von Kossa Staining Protocol

Von Kossa stain was performed using a commercially available kit (HC993161, Merck Millipore, Germany) to identify calcified tissues using silver nitrate (Meloan & Puchtler, 1985). Sections were processed using the same method outlined in Section 2.5. Sections were incubated in 0.1M silver nitrate solution for 20 minutes then under direct light for another 20 minutes. Sections were then washed in tap water for three minutes before being incubated in sodium thiosulphate (20g/L) for five minutes and washed again in tap water for a minute. Sections were then dehydrated and coverslipped by the methods outlined in Section 2.5.

2.9. Alcian Blue Staining Protocol

Alcian blue stain was performed to identify cartilage tissue by reacting with acidic polysaccharides, such as glycosaminoglycan, present in cartilage (Kumar & Kiernan, 2010). The stain was performed at both pH 0.2 and pH 2.5 to observe different staining patterns between the different pH levels and asses which pH would be best suited to these investigations. Following observations, pH 0.2 stain was selected due to a stronger positive stain when exposed to cartilage tissue in comparison to pH 2.5. Alcian blue at pH 0.2 was therefore used on three slides of Gorilla tissue, one slide of bonobo tissue and three slides of giraffe tissue. 0.3g of solid alcian blue (J60122, Alfa Aesar, USA) was mixed with 30ml of 10% sulphuric acid to produce a 1% solution of pH 0.2 alcian blue stain and a pre-mixed solution was used for alcian blue at pH 2.5 (MKCL4108, SIGMA-ALDRICH, USA). For both methods, sections were processed using the same method outlined in Section 2.5. For pH 0.2, sections were incubated with the pH 0.2 alcian blue solution for 15 minutes then blotted dry with filter paper before being rinsed in deionised water for one minute. Sections were counterstained with nuclear fast red for one minute before being washed in tap water for a further minute. For pH 2.5, sections were incubated in 3% acetic acid for five minutes before being incubated in pH 2.5 alcian blue stain for 30 minutes. Sections were washed in

tap water for five minutes then in deionised water for a further one minute before being counterstained by nuclear fast red, again for one minute. For both methods, sections were then dehydrated and coverslipped by methods outlines in Section 2.5.

3. Comprehensive Review of Os Cordis and Cartilago Cordis

This review highlights the similarities and variations in ossa cordis and cartilago cordis prevalence, morphology, histology and anatomical location between differing veterinary species and humans. It also looks at associated factors such as aging and CVD for each species in relation to presence, functional roles and developmental mechanisms that these bone and cartilage structures may play. The potential functions of os cordis and cartilago cordis are presented, from aiding in cardiac contraction and conduction, providing cardiac structure, and protecting components of the heart through to counteracting high mechanical stress. Furthermore, this review discusses the evidence and rationale behind hypotheses' regarding the formation and development of both structures in the different veterinary species and in people.

3.1. Rationale, Aims, Objectives and Hypothesis

The purpose of this review was to collect all relevant published information regarding discoveries of os cordis and cartilago cordis across all species (Figure. 3.1). The collation of this information would allow an easier comparison between species providing a better understanding of os cordis and cartilago cordis as well as allowing trends to be drawn regarding the presentation, formation and function of the two cardiac hyperdense structures.

To obtain all relevant papers, a comprehensive search was carried out across three major databases and a general google search using multiple languages, the methods used are described in Chapter 2.1.

It was hypothesised that os cordis and cartilago cordis would have a similar functions and would develop alongside natural growth or as a result of CVD. The overarching hypothesis regarding the formation of bone tissue was that EO played a role however, the process by which both bone and cartilaginous tissue becomes apparent in the heart was unknown.
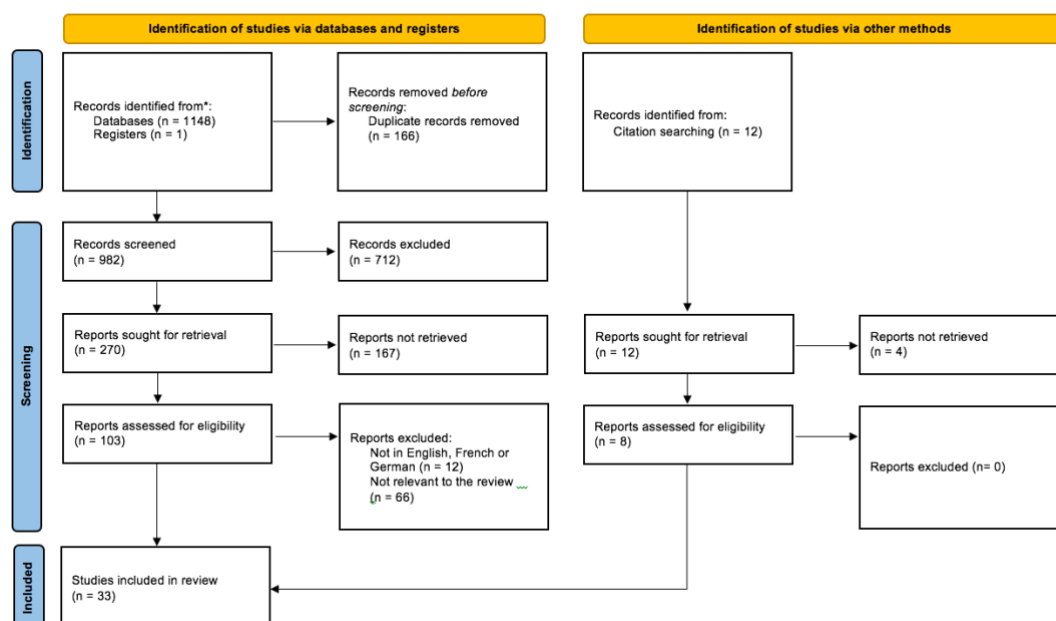
Figure. 3.1. A flow diagram of records found during the literature review in this thesis. The diagram shows the process by which records were eliminated resulting in the remaining studies being included in the comprehensive review written as part of this thesis.

3.2. Results and Discussion

3.2.1. Presentation of Os Cordis

When present, the os cordis is usually associated with the atrioventricular rings and major cardiac septa (interatrial and interventricular) however, the os cordis shows variations between species in its presence, number, size, shape and position (Pour, 2004; Frink & Merrick, 1974; Ghonimi et al. 2014; Daghash & Farghali, 2017). The following information was collated from the literature search undertaken.

3.2.2. Os Cordis in Cattle and Water Buffalos

In cattle (*Bos taurus*), the os cordis has been well documented and each individual may have no bone, one or two (James, 1965; Schmack, 1974; Habermehl & Schmack, 1986; Pour, 2004). Os cordis dextrum (OCD) was found in 100% of 80 hearts investigated (Pour, 2004). The position of the OCD was consistently located on the right side of the heart near the major cardiac septa, beneath, or in some cases extending into the right atrioventricular ring (James, 1965). With reference to the conduction system of the heart the OCD was present above the bundle of His and opposite the AVN (James, 1965). The cranial aspect of the bone sat just below the base of the aorta and the caudal aspect extended with two rami towards the coronary sinus (Pour, 2004; James, 1965). Cattle may also have a second os cordis, os cordis sinistrum (OCS), found in 37.5% of and unspecified cattle breed ('beef'; n= 3 from 8; James, 1965); 80% of Holstein breeds (n=32 from 40) and 20% of native Iranian cattle (n=8 from 40; Pour, 2004). The position of the OCS was relatively consistent across all individuals, presenting in a left

20

sided position comparative to that of the right-sided OCD, and inserting into the left atrioventricular ring. Its average length was 18.43mm (Table. 3.1), smaller than OCD (42.59mm; Table. 3.1; Pour, 2004; James, 1965). One study suggested that the two ossa cordis were connected by cartilage in every instance (James, 1965), however in a more recent study no cartilaginous connection was reported (Pour, 2004).

Similar to cattle, 93% of water buffalo (*Bubalus bubalis*) hearts had two ossa cordis (n=14 from 15; Table. 3.2; Daghash & Farghali, 2017). The OCD in buffalo was comparatively longer than observed in cattle (an average of 52mm, compared to 43mm in cattle). The bone traversed between, and inserted into the right and left atrioventricular rings. The OCS also differed to cattle, rather than inserting into the left atrioventricular ring it was located below the left coronary artery (Daghash & Farghali, 2017).

Breed	Mean Width of OCD - Cra Aspect (mm)	Mean Width of OCD - Cau Aspect (mm)	Mean Length of OCD (mm)	Mean Width of OCS (mm)	Mean Length of OCS (mm)	Reference
Holstein	7.49	18.36	40.85	9.75	19.95	Pour, 2004
Iranian	5.25	10.99	30.92	7.28	17.35	Pour, 2004
Beef (unspecified breed)	4.00	8.40	56.00	11.60	18.00	James, 1965
Average ($\bar{x}$)	5.58	12.58	42.59	9.54	18.43	

Table. 3.1. Ossa cordis morphologies in cattle breeds. Measurements for the 'beef' animals were taken from a scaled image as no reported values were provided (James, 1965). Averages calculated for this study using the published values across breeds and publications.

3.2.3. Os Cordis in Sheep, Goats and Deer

A study examining 25 sheep (*Ovis aries*) discovered an OCD measuring 10-15mm long (Table. 3.2) in all hearts, deep within the interatrial septum. Additionally, an OCS was found within the left atrioventricular ring in ten of the 25 hearts (Frink & Merrick, 1974). Cartilaginous connections were not found between the two bones (where more than one bone was present). Interestingly, the OCD consistently interrupted the normal route of the bundle of His causing it to divert under the bone. The ovine OCS was similar to cattle however, the bone inserts into the anterior cusp of the mitral valve rather than the posterior cusp (Frink & Merrick, 1974; James, 1965). In a separate investigation in 50 Lori-bakhtiari sheep (an Iranian breed), an OCD was found in 52% of hearts, measuring 18.1mm in length on average, in a similar region to previous findings (Table. 3.2; Mohammadpour & Arabi, 2007). Interestingly, in this sheep breed no OCS was found in any of the hearts.

Additionally, a separate investigation found a third bone in 17.9% of right atria investigated using radiography (n=10 of 56; Gopalakrishnan, 2007). However, this study only investigated sheep right atria so it is possible that the third bone was a fragment of the OCD as previously described (Frink & Merrick, 1974).

In a study of 50 native goat hearts (*Capra aegagrus hircus*; Mohammadpour & Arabi, 2007), 44% of adult hearts presented with an OCD. The bone was found in a similar position to the OCD of sheep, near the interventricular and interatrial septa. The OCD in goats was slenderer and elongated than that in sheep and measured 19mm on average rather than 18.1mm in sheep (Table. 3.2). Similar to sheep, no OCS was found in any of the hearts (Mohammadpour & Arabi, 2007).

In the white-tailed deer, a single os cordis was described in four out of ten hearts averaging 20mm in length (Rumph, 1975), comparable to sheep and goats. It contrasts to sheep and goats in its location however, residing at the base of the aorta. In a similar location, a single bone was found in 413 deer hearts collected from hunting in France (Dupuy, 2011). Although it is not stated how many total animals were investigated, and it is not a peer-reviewed publication, this second report does show that os cordis is present in at least some individuals and the report states that the average length of the bone was similar to sheep and goats at 24mm (Table. 3.2).

3.2.4. Os Cordis in the Dromedary Camel

A publication investigating the dromedary camel (*Camelus dromedaries*) observed the presence of a single os cordis in all ten hearts investigated (Ghonimi et al. 2014). The bone had a comparable position to OCD in cattle but no information on bone size was provided in the publication.

3.2.5. Os Cordis in the Chimpanzee

The chimpanzee (*Pan troglodytes*) had a single os cordis, present in three of 16 hearts investigated (Moittie et al. 2020). The position of the bone within the trigonum fribrosum, a similar position to that in cattle and camels, but the bone was smaller comparatively (length $\bar{x}$=6.1mm, Table. 3.2). Despite these similarities with larger mammal ossa cordis it should be noted that all three chimpanzee hearts had idiopathic myelofibrosis, indeed the level of fibrosis was a factor associated with the presence of bone in the heart (Moittie et al. 2020). Therefore, rather than being anatomically normal, as is the case with other larger mammals, the os cordis in chimpanzees is likely to occur in association with CVD.

3.2.6. Os Cordis in the Dog and Cat

Following post-mortems in dogs (*Canis lupus familiaris)* which died suddenly, a single cardiac bone presented in eight of 11 (73%) Doberman pinscher hearts (James & Drake, 1968). The bones were located within the central fibrous body, adjacent to the bundle of His and AVN, however no observations were made on the shape or size of the bone (James & Drake, 1968).

Following CVD (nonsuppurative endocarditis and myocarditis) 63 cat (*Felis catus*) hearts underwent histological investigations (Liu et al. 1975). 58 of the 63 hearts had islands of cartilage present within the central fibrous body and in a further 19 hearts, bone was also found in this region (Liu et al. 1975). The sizes of osseous/cartilaginous foci were not noted and no further observations on the position or the shape of the foci were made.

3.2.7. Os Cordis in the Horse

Cardiac cartilage has consistently been found in horses over five years of age (Schmack, 1974). However, in a four-year-old horse (*Equus caballus*) which died following cardiac arrhythmias, bone foci were observed on necropsy within all three cusps of the left atrioventricular valve. Multifocal bone and cartilaginous foci were also observed throughout the cardiac skeleton (Matsuda et al. 2010). Although this bone was not reported specifically as an os cordis, it is important to note that as well as the chimpanzee, dog and cat, bone has been observed in an equine heart with CVD (Moittie et al. 2020; James & Drake, 1968; Liu et al. 1975; Matsuda et al. 2010).

3.2.8. Os Cordis in the Otter

Another species, to date, with evidenced ossa cordis is the otter (*Lutra lutra*). In one heart two bones were identified, in another heart three were seen and in all other hearts investigated a single os cordis was present (total n= 13; Ergerbacher et al. 2000). The bones measured between 1.5-5mm in length (Table. 3.2) and were irregular in their shape, showing potentially more variation than observations noted in other species. The bones were consistently found within the trigones of the cardiac skeleton but other than this basic trend, the location of the cardiac bones varied widely between individual hearts (Ergerbacher et al. 2000). This variation is unusual in comparison to other mammals therefore further investigation is required. However, it may be due to the unusual cone shape of the otter heart (Ergerbacher et al. 2000).

3.2.9. Os Cordis in the Elephant and Giraffe

A study which examined the hearts of three Asian elephants (*Elephas maximus*) noted that two ossa cordis were found in one of the hearts (Endo et al. 2005). The position of the bones was not reported but, the bones were stated as 80 and 95mm, respectively (Table. 3.2). The cause of death for this individual was unrelated to any heart condition and no evidence of previous CVD was highlighted in the study.

During anatomical investigation of a giraffe heart, a cardiac bone was reported within the right trigone of the cardiac skeleton. No other observations were made about the bone at all (Perez et al. 2008).

Species, bone	Mean Length (mm)	Mean Width (mm)	Mean Depth (mm)	% Occurrence (total hearts investigated)	Reference
W. Buffalo, dextrum	52	13	-	93% (15)	Daghash & Farghali, 2017
W. Buffalo, sinistrum	23	4	-	93% (15)	Daghash & Farghali, 2017
Sheep, dextrum	10 – 15	1 - 2	1 - 2	100% (25)	Frink & Merrick, 1974
Sheep, dextrum	18.1	5.7	2.3	52% (50)	Mohammadpour & Arabi, 2007
Sheep, sinistrum	5.5	5	-	40% (25)	Frink & Merrick, 1974
Goat, dextrum	19	5.2	2.3	44% (50)	Mohammadpour & Arabi, 2007
White tailed deer	20	5	-	40% (10)	Rumph, 1975
Deer (species unknown)	24	-	-	100% (413)	Dupuy, 2011
Camel, dextrum	-	-	-	100% (10)	Ghonimi et al. 2014
Chimpanzee	6.1	6.0	5.0	19% (16)	Moittie et al. 2020
Dog	-	-	-	73% (11)	James & Drake, 1968
Cat	-	-	-	30% (63)	Liu et al. 1975
Horse	-	-	-	100% (1)	Matsuda et al. 2010
Otter	1.5 – 5	-	-	40% (30)	Ergerbacher et al. 2000
Elephant, dextrum	95	-	-	33% (3)	Endo et al. 2005
Elephant, sinistrum	80	-	-	33% (3)	Endo et al. 2005
Giraffe, dextrum	-	-	-	100% (1)	Perez et al. 2008

Table. 3.2. Mean lengths, widths and depths of the os(sa) cordis in all species found with os(sa) cordis excluding cattle (Table 3.1.). The water buffalo, dextrum and sinistrum, and sheep, sinistrum measurements were quoted from a scaled image. All other measurements were quoted directly from the manuscripts noted in the table.

3.2.10. Summary of Os Cordis Number, Location and Morphology in Differing Species

The basic position of os cordis across all species was on the right side of the heart, with the bone associated with the right atrioventricular ring. There was also an obvious relationship between the os(sa) cordis and conduction system of the heart, although this it yet to be fully investigated. Where an OCS was present, it was always smaller than OCD in length and, in most species, associated with the left atrioventricular ring. Variation in the presence of OCS was also noted within the same species, in cattle the OCS was only present in 20% of Iranian breeds in comparison to 80% of Holstein cattle (Pour, 2004). Differences between breeds were also noted in sheep where OCS was found in 40% (10 out of 25) of sheep hearts (breed unknown; Frink & Merrick, 1974) but was not found in any of 50 hearts from an Iranian sheep breed (Mohammadpour & Arabi, 2007). Additionally, Suffolk or Suffolk-cross sheep more commonly developed osteocartilagenous foci in the right atrium in comparison with other breeds (Gopalakirshnan, 2007). This suggests that not only is there variation between species, there may also be breed predispositions towards the presence of OCD/OCS. More investigation into this possibility should be performed as this may correlate with other breed dispositions, especially with reference to CVD.

3.3. Os Cordis Formation and Development

It has been hypothesised that the os(sa) cordis forms via a process known as EO, formation of bone tissue from cartilage, as opposed to IMO, bone being laid down directly onto mesenchyme (Daghash & Farghali, 2017; Ergerbacher et al. 2000; Ghonimi et al. 2014; Moittie et al. 2020; Gopalakrishnan, 2007). Currently, the evidence for EO formation is based mainly on the presence of cartilage associated with os cordis. In water buffalo, the youngest heart investigated (30 days) had no os cordis but did have cartilage present, meanwhile older hearts (up to 5 years old) had an os cordis present in the same anatomical location as the cartilage observed in the calf, thus indicating that the bone may have developed from the cartilage (Daghash and Farghali, 2017). Similar findings were also indicated in deer where cartilage was present instead of bone in younger animals (< 1.5 years; Dupuy, 2011). Additionally, ossification of cartilage was seen histologically in eight of the 30 otter hearts investigated (Ergerbacher et al. 2000). In the chimpanzee, the three individuals with os cordis had cartilage tissue directly attached to the bone, and in one other individual a cartilago cordis was observed in the same location as the ossa cordis observed in the other specimens (Moittie et al. 2020). EO was suggested in the horse where bone trabeculae formed (Matsuda et al. 2010). Additionally, well vascularised cartilage was found around cancellous (spongy) bone in the camel (Ghonimi et al. 2014). In sheep, atrial bone formation was reported as being formed by EO (Gopalakrishnan et al. 2007), but an earlier study did not show any evidence of EO/cartilage (Frink & Merrick, 1974). The only species without any direct evidence of EO are the cat, dog and cattle, however, investigations in dog and cattle hearts did find cartilage in close proximity to bone tissue, again indicating possible EO association (Liu et al. 1975; James, 1965; James & Drake, 1968). The theory of bone formation by EO is therefore supported by cartilage presence in water

buffalo, otters, camels, chimpanzees and sheep as well as supporting evidence in cattle and dogs (Daghash & Farghali, 2017; Ergerbacher et al. 2000; Ghonimi et al. 2014; Moittie et al. 2020; Gopalakrishnan, 2007; James, 1965; James & Drake, 1968).

Naturally, evidence of cartilage in the same location as os cordis (in say younger animals), or cartilage being associated with the os cordis itself is not direct evidence for EO. Indeed, many species contain a cartilago cordis which does not appear to develop into an os cordis. For example, in Syrian hamsters, cartilage has been frequently found in the heart but bone tissue has never been found (Duran et al. 2004; Lopez et al. 2001). The lack of bone development could be related to the size of the animal. In otters it was suggested that the reason for bone formation was related to unusually high mechanical forces on the heart for an animal of that size (Ergerbacher et al. 2000), indeed mechanical forces have been proven to affect the formation of cardiac tissues in general (Bishop & Lindhal, 1999). It is therefore possible that bone never develops in hamsters and other small species because they have a lower blood volume and therefore lower levels of forces within the heart required to pump a lower volume of blood. More investigation into force and os cordis vs cartilago cordis formation should be performed to confirm this, as should there be investigations into larger species with cartilago cordis instead of os cordis, for example the rhinoceros (Erdogan et al. 2014).

Interestingly, there is also very little knowledge pertaining to the initial formation of cartilage, which may eventually develop into os(sa) cordis. In sheep atria, it has been suggested that during heart development, neural crest cells (NCCs) get lodged in the atrial wall and eventually differentiate into cartilage (Gopalakrishnan et al. 2007). This is supported by studies in the quail embryo where NCCs were observed differentiating into cartilage (Sumida et al. 1989). It has also been suggested that cartilage differentiates from NCCs in camels (Ghonimi et al. 2014). However, it is also possible that cartilage forms from different origins. One theory is that cardiac fibrocytes (involved in the formation of the cardiac skeleton, including cartilage) originate from epithelial to mesenchymal transformation (EMT). One study which investigated EMT in the heart stated that during embryonic formation in every cell in the heart undergoes at least one EMT so it is possible that EMT occurs in the formation of cardiac cartilage and subsequent bone (Von Gisse & Pu, 2012). Further research into the origins of cardiac cartilage, especially in relation to cartilago cordis and os cordis, with particular reference to NCCs and EMT, could elucidate the processes involved in os cordis formation.

It is possible that os cordis may develop in a similar fashion to other extra skeletal bones, for example the os penis. In rats and mice, the os penis develops in two parts, the proximal and distal ends, using two different ossification processes. The distal part develops via IMO, before fusing with the cartilaginous proximal part which later develops to bone by EO (Murakimi, 1986). However, os penis development is not consistent between species for example, whereas rodents use both IMO and EO, the canine os penis develops purely by EO (Nasoori, 2020). Os penis therefore shows us that despite evidence of EO in some specimens of ossa cordis, this is no

guarantee that EO is the only process involved in its development. It is even possible that os cordis may develop in a variety of ways dependent on the species it develops in.
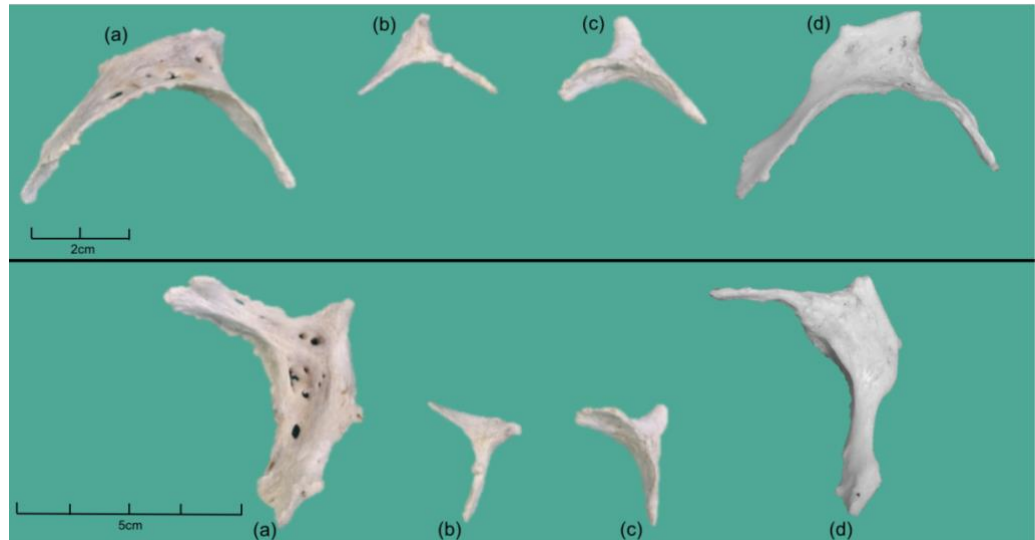
Figure. 3.2. Photographs of four cattle ossa cordis from two different views. (a+d) Images of os cordis dextrum, from two different individuals. (b+c) os cordis sinistrum, from two different individuals.

3.4. Proposed Functions of Os Cordis

Throughout the years, investigations into the mammalian os cordis have suggested two main theories in relation to the function of the cardiac bone(s). In cattle and camels, it has been proposed that the cardiac muscle anchors onto the os cordis improving contraction (James, 1965; Pour, 2004; Ghonimi et al. 2014). Additionally, in cattle, sheep and otters it has been suggested that the os cordis acts to protect the heart from damage in areas of high mechanical stress during systole (James, 1965; Frink & Merrick, 1974; Ergerbacher et al. 2000). Furthermore, in the chimpanzee, horse, cat and dog the presence of os cordis was associated with CVD and the overall function of os cordis in these species was not specifically discussed (Moittie et al 2020; Matsuda et al. 2010; Liu et al. 1975; James & Drake, 1968).

The anatomical position of os cordis may suggest that it plays a mechanical role supporting the heart during contraction. In cattle, it has been noted that the os cordis acts as a supportive structure, similar to the human fulcrum, in order to support the two atrioventricular valves during contraction (James, 1965; Trainini et al. 2020; Pour, 2004). In humans, the cardiac fulcrum, a small tendinous structure within the heart, helps to anchor the myocardial band to aid contraction (Trainini et al. 2020). It is located in front of the aorta, just below the right trigone with the myocardial band originating from it and eventually, inserting back onto its point of origin. Histological analysis of human hearts has also shown the presence of cardiac myocytes inserting into

the human fulcrum as well as the os cordis and the surrounding cartilage in the camel (Trainini et al. 2020; Ghonimi et al. 2014). In camels, it was indicated that the reason for this insertion into the os cordis could help stabilise the heart during contraction and relaxation. As cartilage and bones cells have been observed in the human fulcrum, this has drawn direct comparisons to ossa cordis and cartilago cordis (Trainini et al. 2020). This contrasts to another investigation comparing bovine and human cardiac anatomy which argues that os cordis may not be directly comparable to the human fulcrum, instead the os cordis may be more similar to the right trigone in humans (De Almeida et al. 2019). Despite these contrasting ideas, it is possible that the os cordis has a similar function to the human fulcrum and may aid cardiac contraction.

A number of theories based on differing species have been suggested as to the roles and interactions between mechanical forces and the os cordis. Formation of otter ossa cordis from cartilage may have been triggered by mechanical stress, a theory supported by additional reports which stated mechanical forces trigger the generation of cardiac tissues (Ergerbacher et al. 2000; Bishop & Lindhal, 1999). The anatomical location of os cordis also supports this claim, as they frequently appear in the regions of the atrioventricular rings, between atrioventricular valves or even at the base of the aorta, all areas of the heart which experience the high levels of mechanical pressure (Frink & Merrick, 1974; James, 1965, Dupuy, 2011). Investigation of the sperm whale heart showed there was no os cordis but they also generally lack of dense tissue in the heart (James, 1995). This could be as a result of the whales' buoyant habitat resulting in significantly less mechanical stress. It is therefore reasonable to suggest that the entire pathway of os cordis formation, which may include differentiation of NCCs and subsequent EO, could be triggered by mechanical stress.

It is also important to question whether the os cordis plays protective roles as part of its function. The os cordis may be present to prevent damage in areas of high mechanical stress within the heart (James, 1965; Frink & Merrick, 1974). In cattle, the os cordis is found between the two atrioventricular valves (James, 1965). When both atrioventricular valves contract they put a vast amount of force on the cardiac tissues between these valves therefore the os cordis may exist in order to prevent damage to these tissues (James, 1965). Research investigating camel hearts concurred with this theory, suggesting that the position of OCD enables it to protect the heart during systole (Ghonimi et al. 2014)**.** The ovine OCS is also present in high stress areas between the aortic and mitral valves, this is thought to help prevent shearing forces on sheep heart muscles (Frink & Merrick, 1974). However, the same study noted that the function of the OCD was purely for additional support of the atrioventricular ring and not to protect tissues. The hypothesis that os cordis plays a protective role in the heart has also been used to help explain why ossa cordis are present in some species and not others (Ergerbacher et al. 2000; Daghash & Farghali, 2017; Pour, 2004; Soliman, 2015). With age, the heart is generally more prone to CVD due to the heart becoming less able to resist mechanical forces, therefore more protection of cardiac tissues in older individuals could be offered by the existence of an os cordis (Barasch et al. 2006; Bishop & Lindhal, 1999). Additionally, even the anomaly of the otter

can be explained by this hypothesis, the peculiar cone shape of the otter heart causes more mechanical strain on heart tissues therefore, cardiac bones may be present in the otter to protect the heart against these forces (Ergerbacher et al. 2000). It must be highlighted that not all large, or indeed long living animals have an os cordis though.

The os cordis is well integrated into the conduction system, in close proximity to the AVN and bundle of His (Figure. 3.3; Frink & Merrick, 1974; De Almeida et al. 2019; James, 1965). In sheep the bundle of His runs alongside the os cordis adjacent to the AVN (Figure. 3.3; Frink & Merrick, 1974). This is the same in cattle, where the AVN is only separated from the bone by a layer of adipose tissue (De Almeida et al. 2019; James, 1965). As well as protecting against damage to muscular tissues, the close position of the os cordis to the conduction system of the heart suggests that the cardiac bone may play a vital role in protecting the AVN and bundle of His (James, 1965).
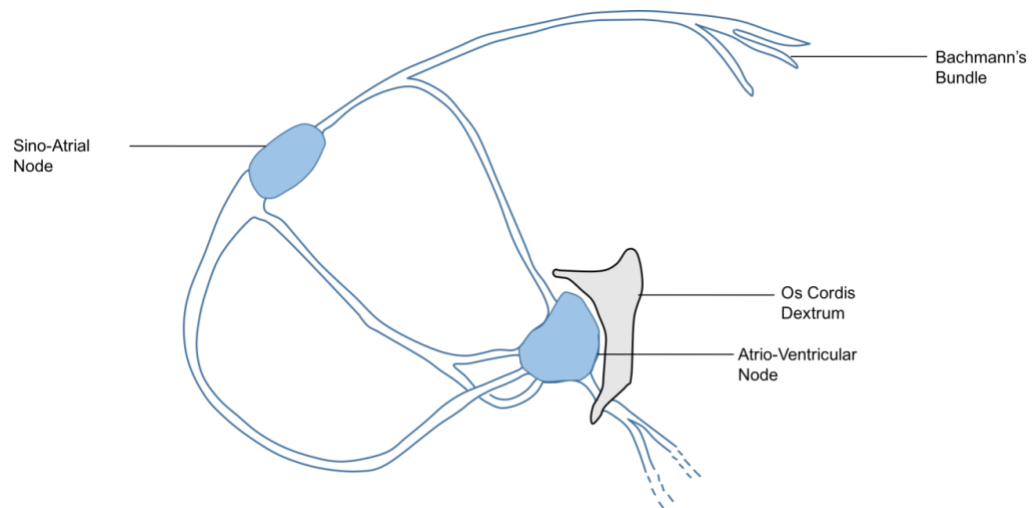
Figure. 3.3. Anatomical drawing of the relative position of the os cordis within the conduction system of the mammalian heart. Adapted from (Hearts Central, 2010).

It is likely that the function of os cordis is to aid in muscular contraction within the heart as well as to protect vital components of the heart. By comparing the os cordis to an arguably better known structure, the human fulcrum, it is clear that the os cordis is likely to play a role, at least in some species, in the contraction of the heart (Trainini et al. 2020). In addition, the position and formation of the os cordis in relation to mechanical stresses indicates a role in the protection of vital cardiovascular structures.

3.5. Correlations Between Os Cordis and CVD

A strong association was identified in chimpanzees between presence of os cordis and IMF. The study found that in the three hearts containing an os cordis, two had severe IMF (level 6) and one had moderate to severe IMF (level 5; Moittie et al. 2020). The reason for bone formation in diseased states may be partially explained by a study which investigated cartilage formation in chickens. This experiment observed cartilage replacing collagen under low

levels of oxygen delivery (ischemia), often seen with CVD (Lehoczky-mona & McCandles, 1964). This is supported in a recent chimpanzee investigation where it was hypothesised that ischemia may have prompted bone formation (Moittie et al. 2020). In dogs, os cordis was found in diseased hearts which presented with bundle of His degeneration caused by ischemia (James & Drake, 1968). It was proposed that the ischemia may have been worsened by the development of os cordis gaining oxygen from a common arterial blood supply with the bundle. The common theme of ischemia throughout these publications may suggest that ischemia causes os cordis formation and, as a result of the cardiac bone being present, the cardiac condition worsens.

Another theory is that bone forms in CVD due to an abnormality in tissue repair, as suggested in the horse, although suggested mechanisms were not given (Matsuda et al. 2010). This theory is supported in incidental findings in rats (Aljinovic et al. 2016). The study focused on left ventricular aneurysm repair and in one of six rats studied scar tissue following the repair showed chondrocytes which developed to bone by EO. However, the aneurysms in this experiment were created by intentional ligation of a coronary artery and to our knowledge bone formation has not been observed due to naturally occurring aneurysms.

Yet another suggestion is that, similarly to natural os cordis development, os cordis can develop as a result of high mechanical forces caused by CVD. In a sample of human cardiac valves 8.75% (103 out of 1,177) contained metaplastic bone (Steiner et al. 2007). The valves examined were from patients who required surgical removal of the valves due to CVD. The formation of this bone is therefore highly likely to be related to conditions caused by disease. Due to the role and location of cardiac valves is likely that bone formation is linked with high mechanical forces.

Alternatively, CVD may generate an environment which prompts endothelial to mesenchymal transition (EndMT). It has been suggested that congenital CVD may activate EndMT causing endothelial cells to differentiate into bone or cartilage cells (Von Gisse & Pu, 2012). This work also showed that endothelial cells develop fibrosis in the heart, similar to what has been seen in dogs, where os cordis eventually developed (James & Drake, 1968). This suggests that os cordis formation seen in animals affected by CVD, may form due to EndMT rather than directly due to ischemia, abnormal tissue repair or high mechanical forces (James & Drake, 1968; Moittie et al. 2020; Matsuda et al. 2010).

One consequence of bone formation is that it may have detrimental effects on the hearts conduction system causing sudden death. In two children (aged 6 months and 24 months) cartilaginous foci were found within the central fibrous body (Ferris & Aherne, 1971). In both cases the patients had died suddenly and it was suggested that cartilaginous foci may have caused dysfunction of the AVN, causing sudden death (Ferris & Aherne, 1971). In dogs who had sudden death, bone formation was present in eight of 11 cases, and due to the proximity of os cordis to the bundle of His, it is possible that the bone had detrimental effects on the hearts conduction system (James &

Drake, 1968). Further investigations into cats shows that os cordis or cartilaginous foci compressed the nodes of the heart causing lysis and granulation of nodular fibers (Liu et al. 1975). When discussing sudden death, which had occurred in 25% of the cats studied, an alternative hypothesis was suggested: Sudden death could be attributed to a lack of blood supply to the brain, caused by failing nodular activity within the heart (Liu et al. 1975). The suggestion that bone formation in the heart may have detrimental effects is well supported by findings regarding cartilago cordis. A study which analysed the AVN of horses, dogs and pigs showed that when cartilage is present within cardiac skeleton the AVN reduced in size and the levels of collagen increased within the node, decreasing the size of the nodes functioning P cells (Gomez-torres et al. 2021). These effects are highly likely to reduce the function of the node.

In summary, CVD seems to be associated with, or may even initiate, cardiac bone development. This may be related to unfavorable conditions such as ischemia, abnormal tissue repair or high mechanical forces as a result of CVD. Subsequently, once bone has formed, disease progression occurs either by generating unfavorable conditions and/or by physical disruption of the conduction system of the heart. However, whether, and how, disease progression results in sudden death requires further investigation.

The initiation factors for cardiac bone formation via EO have yet to be determined or discussed in publications but, by combining observations made in sheep, whales, water buffalo and quails, one possible mechanism of EO initiation is likely to be high mechanical forces on the heart (Gopalakrishnan et al. 2007; James, 1995; Daghash & Farghali, 2017; Sumida et al. 1989). Studies on diseased hearts in chimpanzees, humans and dogs have suggested an equally likely hypothesis that EO is triggered by unfavorable cardiac conditions caused by disease, including high mechanical forces (Moittie et al. 2020; Steiner et al. 2007; James & Drake, 1968). The literature suggests that in some species (cattle, sheep, camels, water buffalo and otters), the os cordis will form naturally if development of the heart produces mechanical stresses significant enough to trigger bone development (James, 1965; Frink & Merrick, 1974; Ghonimi et al 2014; Daghash & Farghali, 2017; Ergerbacher et al. 2000). Additionally, in species which do not develop cardiac bone naturally, such as chimpanzees, humans, horses, cats and dogs, bone may develop due to unfavorable cardiac conditions originating from cardiac disease. In these cases, further research could show that preventing bone development could markedly reduce the progression of disease and in some cases may prevent sudden death.

3.6. Correlations Between Os Cordis and Age
Os cordis presence and size have been investigated using morphological and histological analysis, often comparing hearts of varying ages. In otters, evidence of bone and/or early ossification was observed in 12 hearts, only one of which was characterised as sub-adult compared to all other hearts being either adults or their ages unknown (Table. 3.3; Ergerbacher et al. 2000). In water buffalo, the os cordis was not seen in the heart of a one-month old calf

however in buffalo, two ossa cordis were present in all 14 hearts from individuals aged between three and five years old (Table. 3.3; Daghash & Farghali, 2017). Cardiac bone has been detected in adult sheep hearts but only cartilage was found in the heart of a four-month old fetus (Table. 3.3; Nabipour & Shahabodini, 2007; Frink & Merrick, 1974). A distinct positive correlation was found between age and the length of os cordis in deer, progressing from a mean length of 17.5mm at 1.5 years old to 35.8mm at 13.5 years old (Dupuy, 2011). Cattle studies have shown that although the bone is present, os cordis size varies between two different age groups (<1year and 1-2years); the OCD increased from 36.98 to 37.61mm (mean average respectively) and OCS increased from 8.20 to 13.83mm (mean average respectively; Table 3.3; Pour, 2004). In 11 Doberman Pincher dog hearts, three hearts were from individuals under three years of age who contained no os cordis whereas, in the remaining eight hearts, all aged over three years, bone was present (Table 3.3; James & Drake, 1968). In healthy horses, cartilage does not typically develop until after 5 years of age (Schmack, 1974), however following cardiac arrhythmias, indicative of cardiac disease, the horse os cordis has developed at four years of age (Matsuda et al. 2010). The presence of an os cordis was not specifically related to age in chimpanzees, cats or camels however, none of these studies investigated any juvenile hearts (Moittie et al. 2020; Liu et al. 1975; Ghonimi et al. 2014).

It is clear that generally the presence and formation of os cordis is age dependent. In some species, os cordis development appears to be a physiologically normal event as the bone develops with age. In contrast, cardiac disease could be a contributing factor regardless of age. Therefore, future investigations looking at hearts of varying ages is vital in order to understand changes in the heart, due to both age and disease, which could be responsible for the formation and development of os(sa) cordis.

Species (Age)	% Presence of bone (number of hearts in age bracket)		Reference
	OCD	OCS	
Holstein Cattle (<2 years)	100% (40)	80% (40)	Pour, 2004
Iranian Cattle (<2 years)	100% (40)	20% (40)	Pour, 2004
Water Buffalo (1 month)	0% (1)	0% (1)	Daghash & Farghali, 2017
Water Buffalo (3-5 years)	100% (14)	100% (14)	Daghash & Farghali, 2017
Sheep (Fetus)	0% (5)	0% (5)	Nabipour & Shahabodini, 2007
Sheep (Unknown Age)	100% (25)	40% (25)	Frink & Merrick, 1974
Sheep (1.5-2 years)	52% (50)	0% (50)	Mohammadpour & Arabi, 2007
Elephant (21-38 years)	0% (2)	0% (2)	Endo et al. 2005
Elephant (56 years)	100% (1)	100% (1)	Endo et al. 2005
Goat (1.5-2 years)	44% (50)		Mohammadpour & Arabi, 2007
White Tailed Deer (6 months – 4.5 years)	40% (10)		Rumph, 1975
Deer (1–14 years	100% (413)		Dupuy, 2011
Camel (7-9 years)	100% (10)		Ghonimi et al. 2014
Chimpanzee (10-59 years)	18.8% (16)		Moittie et al. 2020
Dog (≤9 weeks)	0% (2)		James & Drake, 1968
Dog (3 years)	0% (1)		James & Drake, 1968
Dog (≥3.5 years)	100% (8)		James & Drake, 1968
Cat (Adult)	30% (63)		Liu et al. 1975
Horse (4 years)	100% (1)		Matsuda et al. 2010
Otter (Juvenile, <1 years)	0% (3)		Ergerbacher et al. 2000
Otter (Sub-adult, 1-2 years)	11.1% (9)		Ergerbacher et al. 2000
Otter (Adult, >2 years)	69.2% (13)		Ergerbacher et al. 2000
Otter (Unknown Age)	40% (5)		Ergerbacher et al. 2000
Giraffe (Unknown Age)	100% (1)		Perez et al. 2008

Table. 3.3. Percentage prevalence of os cordis dextrum and, where present, sinistrum in 13 different species, and how it varies across different ages of those species.

3.7. Presentation of Cartilago Cordis

In Syrian hamsters (*Mesocricetus auratus*), a cartilago cordis was present in 142 of 567 hearts, all within the right trigone near to the interventricular and interatrial septa. In addition, calcification was observed in 23% of the cartilago cordis (Table 3.4; Duran et al. 2004). A different study showed lower numbers, only 40 of 351 Syrian hamsters had cardiac cartilage (Table 3.4; Lopez et al. 2001). Chinchillas (*Chinchilla lanigera*) had cartilago cordis in all 30 hearts investigated, located within the left atrioventricular valve and left atrioventricular opening (Warchulska et al. 2016). Early reports of the platypus (*Ornithorhynchus anatinus)* heart make reference to a cartilago cordis beside the AVN and bundle however, no other details were provided on this structure (Davies, 1931). Additionally, pigs (*Sus scrofa domesticus*) are known to have cartilage within their cardiac skeleton, in a study which examined eight atrioventricular zones from pig hearts, three contained hyaline cartilage and one more contained fibrocartilage (Gomez-Torres et al. 2021). Only the atrioventricular zone was investigated in this study and the shape nor size was commented on. Due to the sampling site used in this investigation it was possible to deduce that the cartilago cordis in pigs resides close to the AVN. In a smaller species, the mouse (*Mus musculus*), cartilaginous foci have been found using histological techniques within the atrioventricular valves (Icardo & Colvee, 1995). This fibrocartilage was observed at all ages in the study of 15 mice and so was thought to be a naturally occurring event.

Cartilago cordis has also been found in 11 of 42 species of snake (*Serpentes*; numbers of hearts examined in each species was not noted; Table. 3.4). The position of cartilago cordis in snakes varied widely in comparison to hamsters, but was found within the aorticopulmonary septum, between the pulmonary vein and aorta (Young, 1994). The cartilage measured 0.3-0.55mm in length and the shape of the cartilago cordis varied across the 11 species however, three common shapes were described as disk, rod and block (Young, 1994). An interesting trend noted within snakes was that cartilago cordis was found mostly in terrestrial species. In iguanas (*Iguana iguana*), cartilage tissue was found within the cardiac skeleton, no other observations were made regarding the position, size or frequency of this finding (Jurado et al. 2006). Spanish terrapins (*Mauremys leprosa*) were also found to have cartilaginous tissue within the cardiac skeleton with all 8 post-partum specimens presenting with a cartilago cordis within the proximal region of the aorticopulmonary septum (Lopez et al. 2003). Additionally, in seven specimens (all aged 18 months or older), a second cartilago cordis was found within the right sided aorta of the reptiles (Lopez et al. 2003). In another chelonian, the green sea turtle (*Chelonia mydas*) fibrocartilage was found within the cardiac skeleton, and hyaline cartilage was found in the atrioventricular valves of the turtle (frequency, shape and size of this finding was not noted; Braz et al. 2015).

In 28 adult chickens (*Gallus gallus domesticus*) and 10 adult quails (*Coturnix coturnix*) all had a cartilago cordis in a similar cardiac position to that observed in snakes, in front of the aorticopulmonary septum (Table 3.4; Lopez et al. 2000). Furthermore, in 71% of these adult chickens and 40% of the adult quails, the cartilage extended into the aortic leaflet of the aorta's semi-lunar

valve. This was confirmed by a later paper which observed cardiac cartilage within the aortic ring, although the frequency of this was not stated (Sasasn et al. 2015). Cartilago cordis has also been discovered in a larger species, the white rhinoceros (*Ceratotherium simum*; Table 3.4; Erdogan et al. 2014). The study only investigated one heart however, one cartilago cordis was present within the right trigone of that heart. No other observations were made regarding the size, shape or position of this cartilago cordis. Cardiac cartilage in horse (*Equus caballus*) has been found consistently in individuals over five years of age in close proximity to the septa of the heart, measuring 25-35mm in length (Schmack, 1974; Habermehl and Schmack, 1986). A cartilage cordis sinister (cherry-stone size) has regularly been found in horses older than 5 years and an accessory cardiac cartilage (apple-seed size) was also found in some horses older than seven years of age but no specific lengths or positions were noted.

Species investigated	% Hearts (H) or Species (S) with Cartilago Cordis (total number investigated)	Reference
Hamster	25.0% (H = 567)	Duran et al. 2004
Hamster	11.4% (H = 351)	Lopez et al. 2001
Snake	26.2% (H = 58, S = 42)	Young, 1994
Chicken (Adult)	100% (H = 28)	Lopez et al. 2000
Chicken (Sub-adult ≤ 7days)	0.00% (H = 9)	Lopez et al. 2000
Quail (Adult)	100% (H = 10)	Lopez et al. 2000
Quail (Sub-adult ≤ 7days)	0.00% (H = 12)	Lopez et al. 2000
Rhinoceros	100% (H = 1)	Erdogan et al. 2014
Terrapin (post partum)	100% (H = 8)	Lopez et al. 2003
Chinchilla	100% (H = 30)	Warchulska et al. 2016
Platypus	Unknown	Davies, 1931
Pig	50% (H = 8)	Gomez-Torres et al. 2021
Mouse	100% (H = 15)	Icardo & Colvee, 1995
Iguana	Unknown	Jurado et al. 2006
Green Sea Turtle	Unknown	Braz et al. 2015
Horse (> 5 years)	Unknown	Schmack, 1974; Habermehl & Schmack, 1986

Table. 3.4. Percentage prevalence of cartilago cordis in seven different species at various ages.

3.8. Cartilago Cordis Formation and Development

Cardiac cartilage is known to be of NCC origin (Sumida et al. 1989). Further investigation into cartilago cordis in hamsters, chinchillas, chickens, terrapins and quails concur with this theory and noted that NCCs produce the precursors to cartilage (Duran et al. 2004; Warchulska et al. 2016; Lopez et al. 2001; Lopez et al. 2003; Lopez et al. 2000). The trigger for cartilage development is unknown but it has been suggested that high mechanical forces, although not the sole reason for development, may trigger cartilage formation to counteract high mechanical stress in specific areas of the heart such as the atrioventricular valves (Warchulska et al. 2015). Cartilago cordis also seems to form early in life, one investigation in hamsters stated that most cartilage formation occurs within 40 days post-birth (Duran et al. 2004). Furthermore, cartilage tissue has been observed in terrapin embryos (Lopez et al. 2003). This early development of cartilage is vastly different to bone formation which seems to take longer to develop. Another contrast to bone is that generally cartilage prevalence seems to deteriorate in old age, whereas bone continues to develop. In hamsters 55.2% (32 out of 58) of hearts aged 41-80 days-old had cartilage present whereas this proportion was significantly lower in hearts over 80 days-old, decreasing to 39.8% (70 out of 176; Duran et al. 2004). The early development, and late degradation, of the cartilago cordis suggests that cartilage formation in the heart is present in normal physiology and is not a direct result of aging.

3.9. Proposed Functions of Cartilago Cordis

Having looked at the potential functions of os cordis, it is of interest as to whether cartilago cordis plays similar roles. In snakes and hamsters, it has been suggested that the cartilago cordis is present to aid myocardial contraction (Duran et al. 2004; Young, 1994). In snakes, due to the vast variation in the shape and size of cartilago cordis across species it was difficult to interpret function but it was suggested the tissue likely supports the roots of the aorta and pulmonary vein (Young, 1994). In contrast, the hamster cartilago cordis was strongly linked to a role within myocardial contraction due to its position near the major cardiac septa, a similar position to os cordis and the human fulcrum (Duran et al. 2004; Trainini et al. 2020). In addition to aiding contraction, it has been suggested that in chinchillas, chickens, quails, snakes, terrapins, green turtles and hamsters that cartilago cordis helps to support the heart in areas of high mechanical stress, a similar function to that proposed with os cordis (Warchulska et al. 2015; Lopez et al. 2000; Young, 1994; Lopez et al. 2003; Braz et al. 2015; Duran et al. 2004). High levels of mechanical stress are put onto the leaflets of the atrioventricular valves during contraction. This is the precise region where cartilaginous tissue was found in the chinchilla, therefore it was suggested that the presence of cartilage tissue is significant in counteracting these forces (Warchulska et al. 2016). Hyaline cartilage also found in the atrioventricular valves in green sea turtles was suggested to play a role in resisting mechanical forces against those valves during pressure changes as the turtle dives below sea level (Braz et al. 2015). The aorticopulmonary septum in the hearts of chickens and quails is a region of high mechanical stress and it was suggested that cartilago cordis acts to support the heart against these forces (Lopez et al. 2000). Despite presenting

in a different position, similar findings were reported in hamsters where cartilago cordis was noted to support the heart under mechanical stress. In addition, cartilage in hamsters showed more calcification when exposed to greater mechanical stresses, these findings were similarly supported in an investigation of cartilage found in otter hearts (Duran et al. 2004; Ergerbacher et al. 2000). Like os cordis, the cartilago cordis may also provide protection to the hearts vital structures. Observations made in platypus show cartilago cordis resides in contact with the AVN suggesting is may form to protect this vital tissue (Davies, 1931).

The cartilago cordis positioning in hamsters and chinchillas is similar to that of the os cordis (Duran et al. 2004; Warchulska et al. 2016), but in chickens, quails and snakes the cartilago cordis position varies vastly in comparison to the os cordis in other species (Sasasn et al. 2015; Lopez et al. 2000; Young, 1994). The function of cartilago cordis has been proposed to be similar to that of os cordis, functioning to aid stability and contraction within the heart. Formation of cartilago cordis in hamsters, chickens and quails indicates that NCCs develop into cartilage which may then lead into EO, a very likely pathway for os cordis development (Warchulska et al. 2016; Duran et al. 2004; Lopez et al. 2001; Lopez et al. 2000).

3.10. Relationship Between Genetics and Os(sa) Cordis and Cartilago Cordis.

By comparing instance of os cordis, cartilago cordis and ossa cordis of varying number with phylogenetic data it is possible to demonstrate that the appearance of os(sa)/ cartilago cordis may be linked to genetics. Species within the same order frequently present with the same hyperdense structures within the heart (Figure. 3.4). In particular, the *Atriodactyla* order seems to have a multitude of species within it presenting with os(sa) cordis (Figure. 3.4). Despite this, it is also plausible that os(sa)/cartilago cordis development occurs as a result of cardiac conditions which are themselves similar between species within an order. Therefore, occurrence of os(sa)/ cartilago cordis is not a direct result of genetics but rather indirect via cardiac conditions which are predisposed by genetics. Despite extensive findings within this study, the role of genetics in the occurrence of cartilaginous and osseous structures within the heart cannot be fully understood without the full investigation of all species within an order with intent to find or rule out presence of os(sa)/ cartilago cordis in each instance.
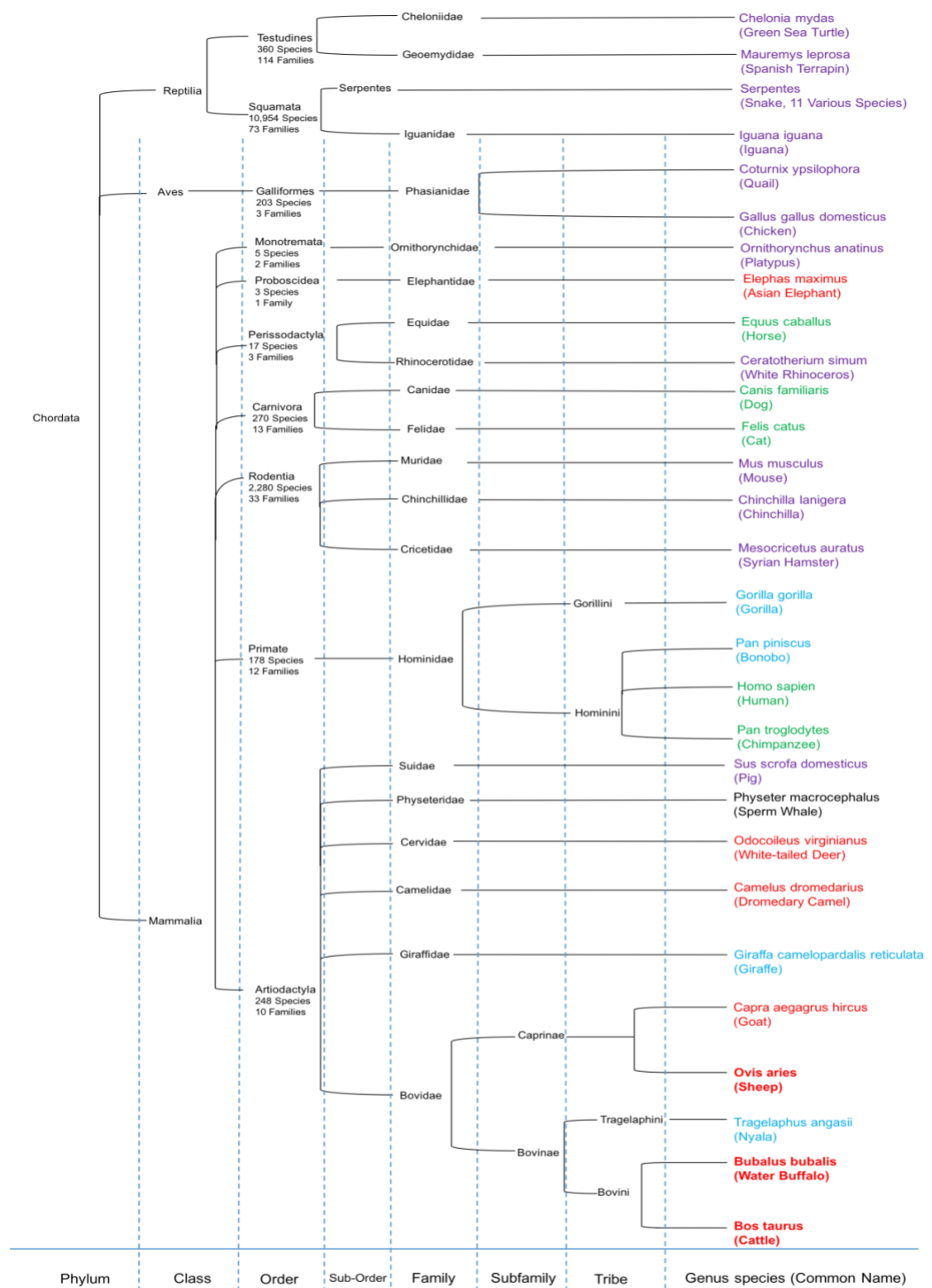
Figure. 3.4. Phylogenetic tree cross referenced with information from this literature review of 35 notable species categorised into those with os cordis, two ossa cordis, os(sa) cordis associated with cardiovascular disease and those without os cordis alongside the four species investigated in this study (Chen et al. 2019).

3.11. Conclusions

After collecting data on all previously reported os(sa) cordis and cartilago cordis, the main hypotheses and theories regarding the formation and function of these structures were collated. The formation of cartilago cordis was largely thought to be a development of NCCs, although evidence is yet to be fully demonstrated. It is also likely that premature os cordis growth also starts with NCC to cartilage formation which then develops to bone by EO. Os cordis and cartilago cordis likely perform similar functions to protect vital structures within the heart from high mechanical forces and, at least in some species, has a role to aid in myocardial contraction much like the human fulcrum. It is also clear that in most cases os(sa)/ cartilago cordis appear within the trigones of the heart in close affiliation with atrioventricular valves, although there are distinct exceptions to this positioning. Although it is likely that genetics plays a role in the appearance/absence of os/cartilago cordis, for this to be confirmed all species in a direct line of evolutionary links should be investigated and analysed for genetic changes which may show associations between the presence or absence of os cordis or cartilago cordis development.

4. Novel Discovery of Ossa Cordis in the Nyala and its Comparison to Os Cordis in a Similar Species, the Giraffe

This chapter shows a novel investigation into a single nyala (*Tragelaphus angasii*) and giraffe (*Giraffa camelopardalis reticulata*) heart. The nyala is a relatively large bovid species of antelope found in south eastern Africa and is a member of the *Bovidae* family (*Bovinae* subfamily), along with water buffalo and cattle (Figure. 4.1, Chen et al. 2019). Despite also being a ruminant and originating from the same order, *Artiodactyla*, giraffes come from a different family to nyala, the *Giraffidae* (Figure. 4.1, Chen et al. 2019). By investigating these two species alongside phylogenetic data, new hypotheses can be introduced pertaining to the presence of os(sa) cordis and their links to evolutionary processes.

4.1. Rationale, Aims, Objectives and Hypothesis

Investigating the nyala and giraffe for hyperdense cardiac structures allowed us to enhance our understanding of cardiac anatomy within these species. Additionally, investigations into a bovid and non-bovid within the *Artiodactyla* order could provide more information on the formation, function and presentation of os(sa) cordis, across other species which have os(sa) cordis. The more species investigated in relation to os cordis, the more one can support or deny hypotheses regarding the bones presence, formation and function.

The study of both species aimed to identify whether any hyperdense structures were present within either heart, and if present, aimed to identify any hyperdense tissues and to provide further evidence as to their formation and function within the cardiovascular system. To do so, each heart underwent

multiple macroscopic investigations using dissection, microCT scans, histological staining using different stains and subsequent microscopy.

It was hypothesised that due to their evolutionary background both species were highly likely to have at least one os cordis, and that they may display evidence of EO. It was also hypothesised that the position of the bone(s) would be in the regions of the interatrial and interventricular septa, similar to most species previously identified as having os(sa) cordis, and that this position could be indicative of a role to protect vital structures due to high levels of cardiac mechanical stress.

4.2. Introduction

No previous studies have investigated the nyala for presence of hyperdense tissues within the heart. Only one study has commented on the presence of a single bone in the giraffe heart, however they only commented on its existence and showed no evidence of histological or radiographical investigations, and did not comment on its size or location (Perez et al. 2008).

Os(sa) cordis have been found in multiple species from the *Artiodactyla* order. Studies focusing on water buffalo and cattle from the *Bovinae* subfamily (Figure. 4.1), have found OCD in all adults, alongside OCS in most hearts (Daghash & Farghali, 2017; Pour, 2004). Studies investigating the hearts of sheep and goats, from the *Caprinae* subfamily (Figure. 4.1) have found OCD with a prevalence of around 50% (52% of 50 sheep and 44% of 50 goats) and no evidence of OCS (Mohammadpour & Arabi, 2007). However, an alternative study has found OCD in all of 25 sheep hearts, ten of which also had OCS (Frink & Merrick, 1974).

Other non-bovine families from the *Artiodactyla* order (Figure. 4.1) have also presented with ossa cordis. A single os cordis was reported in all ten camels studied previously (family: *Camelidae*; Figure. 4.1; Ghonimi et al. 2014). Additionally, OCD only has been found in white-tailed deer (family: *Cervidae;* Figure. 4.1), at the base of the aorta in four out of ten hearts (Rumph, 1975). Furthermore, cartilago cordis have been observed in pig hearts (family: *Suidae*; Gomez-torres et al. 2021). Contrasting to other members of the *Artiodactyla* order, a study which investigated the hearts from six adult sperm whales (family: *Physeteridae;* Figure. 4.1) found no os cordis, cartilaginous tissue or even a central fibrous body (James et al. 1995). The buoyant aquatic environment of sperm whales was thought to be a contributing factor in their lack of hyperdense tissues.
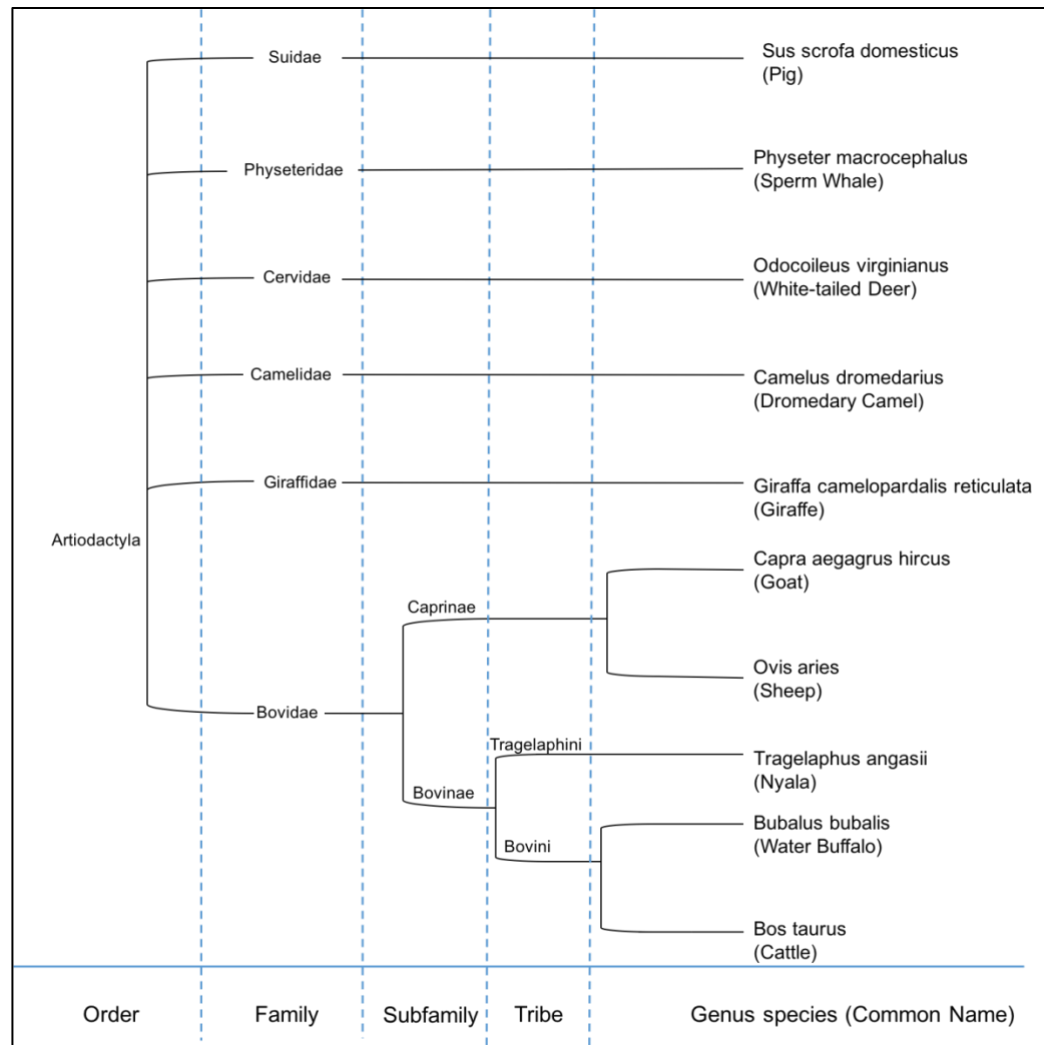
Figure. 4.1. Phylogenetic tree demonstrating how the camel, goat, sheep, water buffalo, sperm whale, deer, pig and cattle are related to the nyala and giraffe (Chen et al. 2019).

4.3 Results

MicroCT and histological investigations (see Chapter 2. Materials and Methods) into the nyala heart discovered four ossa cordis, whereas a single os cordis was found in the giraffe. The giraffe os cordis and two of the nyala ossa cordis were present within the regions of the cardiac septa, while the other two nyala ossa cordis resided at the base of the aorta and the right ventricular wall. In the giraffe os cordis and the largest nyala os cordis, cartilage tissue was present next to bone. Additionally, chondrocytes were observed displaying signs of EO, invading into bone tissue. The results below show how these structures and characteristics were identified.

4.3.1 Preliminary Macroscopic and Pathology Investigations

After death in Twycross Zoo and subsequent post mortem by the Laboratory Dedicated to Zoo, Exotic and Wildlife Pathology each heart underwent detailed macroscopic and histopathological examinations. The female nyala was diagnosed with pneumonia, tracheitis, rumenitis and reticulitis as well as haemosiderosis of the liver, spleen and lymph nodes. The male giraffe showed subepicardial heart hemorrhage as well as chronic nephritis of the kidney. Neither species had any CVD reported prior to death.

4.3.2. X-ray Computed Microtomography

By utilising microCT it was possible to produce clear images of the nyala and giraffe heart tissues as well as any hyperdense tissues within the heart. This technique has only been used once (in the chimpanzee) to investigate ossa cordis, as other older studies have used radiography or simply dissection (Moittie et al. 2020). Hyperdense cardiac tissues, which may be bone, calcification or cartilage, is displayed as bright white on microCT scans. In contrast, medium density tissue such as myocardium and hypodense tissues such as the cardiac chambers are visualised as shades of grey to black.

Four hyperdense structures were observed in the nyala heart and the dissected sample of giraffe heart tissue was made up almost entirely of hyperdense tissue (Figure. 4.2a+b, Figure. 4.3). Using computerised imaging techniques enabled observation of trabeculation within all of the hyperdense structures from both the nyala and giraffe, this trabeculation is a characteristic feature of bone (Figure. 4.2c). As a result of trabeculation the hyperdense structure in the giraffe sample could be confirmed as a rectangular shaped bone which measure 18.5mm in length (Table. 4.1). The discovery of four bones in a single heart presented as a unique feature. Previously the maximum number of ossa cordis discovered in any species was two in a single heart. Since only two ossa cordis in a single heart have been previously identified and named, the nomenclature of four ossa cordis has never been suggested. We therefore propose the following nomenclature. The largest t-shaped structure, depicted in blue (5; Table. 4.1), was present within the right side of the heart within both the atrial and ventricular walls with a branch extending towards the interatrial septum, and therefore we propose it should be regarded as OCD (Figure. 4.2a). The elongated bone depicted in yellow (6; Table. 4.1) was present at the base of the aorta and will be referred to as the os cordis superior sinistrum. Finally, the two triangular bones depicted in orange (1) and green (2), which were present in the regions of the interatrial and interventricular septa, will be known as the os cordis intermedius sinistrum and os cordis inferior sinistrum respectively (Table. 4.1; Figure. 4.2a).
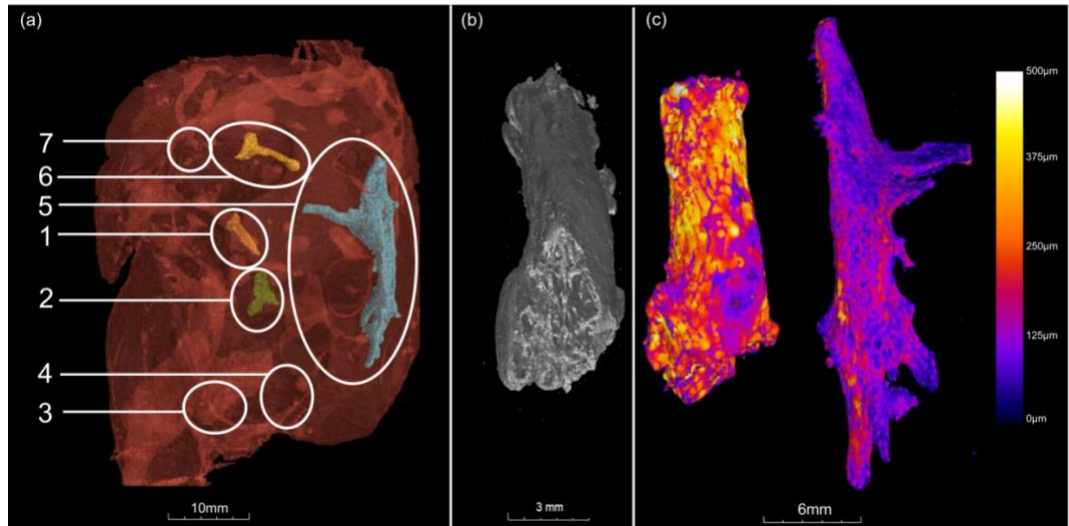
Figure. 4.2. MicroCT scans, at 120 kV and 200 µA, of the nyala heart and giraffe hyperdense tissue found during dissection alongside local thickness measurements (0 - 500µm) of the largest nyala hyperdense structure and the hyperdense structure found in the giraffe. (a) A microCT scan of the nyala heart with sample locations indicated, the scan shows heart tissue in red, and four ossa cordis depicted in assorted colours. (b) A microCT scan of the giraffe os cordis. (c) A local thickness measurement heatmap of the largest nyala os cordis (right) and the giraffe os cordis (left). Scale bars represent 10mm (a), 3mm (b) and 6mm (c).

Sample	Length (mm)	Width (mm)	Depth (mm)
Nyala 5 (blue)	26	11	12
Nyala 6 (yellow)	12	4	1.5
Nyala 1 (orange)	5	3	1.5
Nyala 2 (green)	6	4	2
Giraffe	18.5	7	7

Table. 4.1. A table of measurements taken of each of the four nyala os cordis labelled by their sample number and the single giraffe os cordis. The table shows the length, width and depth of each bone in mm.
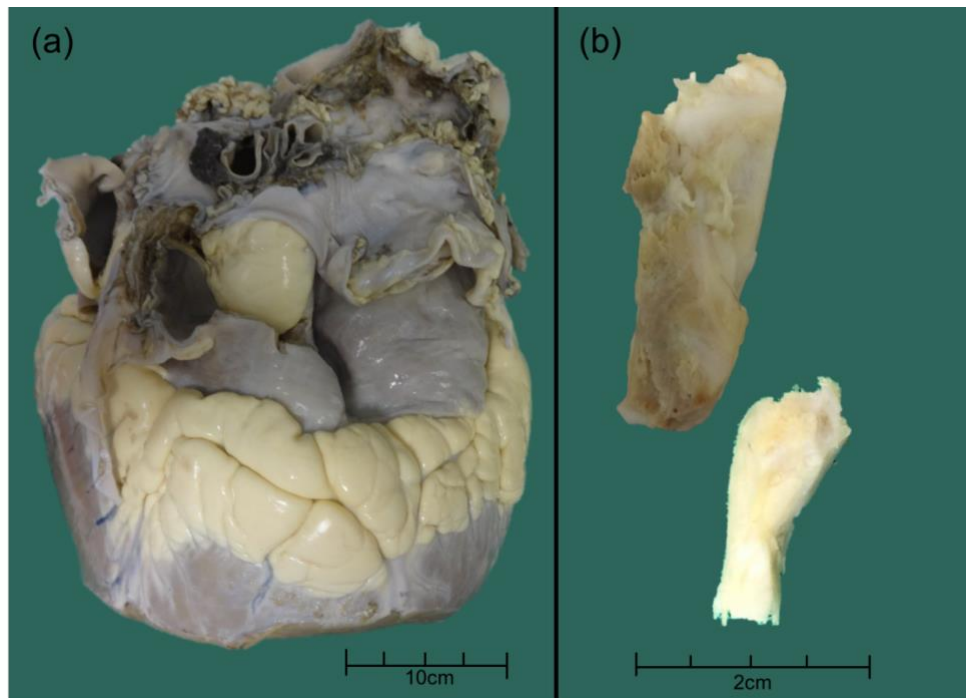
Figure. 4.3. Photographs of prosections taken during the dissection of the giraffe heart. (a) Whole heart prior to dissection. (b) major hyperdense structure of interest taken from the interatrial septum (above) and the same structure after soft tissues had been removed (below). Scale bars represent 10cm (a) and 2cm (b).

4.3.3 Histological Analysis of Heart Tissue

As described in the materials and methods (Section 2.3), the nyala and giraffe samples were processed, sectioned and histological stains undertaken. The nyala had 7 paraffin blocks (referred to as 1-7) and the giraffe had 5 (referred to as A-E).

In both hearts, the endocardial and pericardial layers of the heart were observed as well as cardiomyocytes within a typically striated myocardium in horizontal and vertical planes (Figure. 4.4a) alongside frequently apparent blood vessels. In three nyala samples (Sample 1, 2 + 3; Figure. 4.2) the myocardium looked morphologically abnormal as the cardiac tissue contained an atypically high number of erythrocytes and adipocytes, in addition to a waved pattern across cardiac muscle fibers (Figure. 4.4b+c). As well as these abnormalities, a non-uniform tissue type was also observed in the nyala (Sample 2), thought to be the bundle of His (Figure. 4.4d). In the giraffe however, H+E histological investigations of the myocardium showed no abnormalities, these results were consistent with the preliminary investigations by the pathologist.
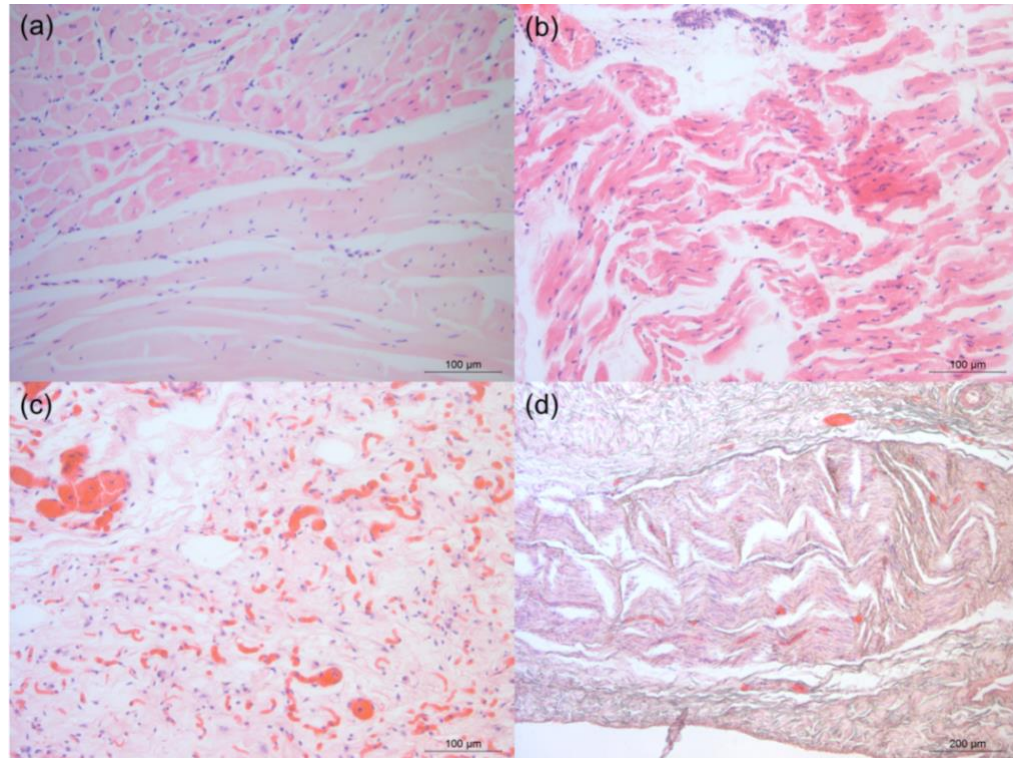
Figure. 4.4. Photomicrographs of the H+E stained myocardium from the nyala and giraffe which demonstrated diseased myocardium. (a) Giraffe (Sample E) displaying typical myocardium in both horizontal (below) and vertical (above) planes. (b, c) Nyala (Samples 1+2) showing diseased myocardium and waved tissue. and additionally showed high erythrocyte (Sample 1) and adipocyte numbers (Sample 2). (d) Non-uniform tissue in the nyala thought to be the bundle of His. Scale bars represent 100µm (a-c) and 200µm (d).

4.3.4. H+E Histological Analysis of Hyperdense Structures in Nyala and Giraffe.

In four nyala cardiovascular tissue samples (Samples 1, 2, 5 and 6) and in the giraffe (Samples B, C and D) bone tissue was confirmed by assessing its morphological appearance when stained with H+E. In the nyala samples which contained bone, hematopoietic cells were observed within a distinct bone marrow (Figure. 4.5a). The giraffe os cordis was morphologically similar to that of the nyala aside from its marrow which contained no hematopoietic cells, it instead was composed of adipose tissue (Figure. 4.5b). Blood vessels were seen frequently on the periphery of the bone tissue and on occasion within bone marrow itself in both the nyala and giraffe (Figure. 4.5e+f). In addition to bone marrow and blood vessels, cartilage was present in the nyala (Sample 2) and in all of the samples which contained bone in the giraffe. Cartilage was identifiable through H+E stains by visualisation of the chondrocytes which were seen directly adjacent/invading into bone tissue, indicative of EO (Figure. 4.5c+d).
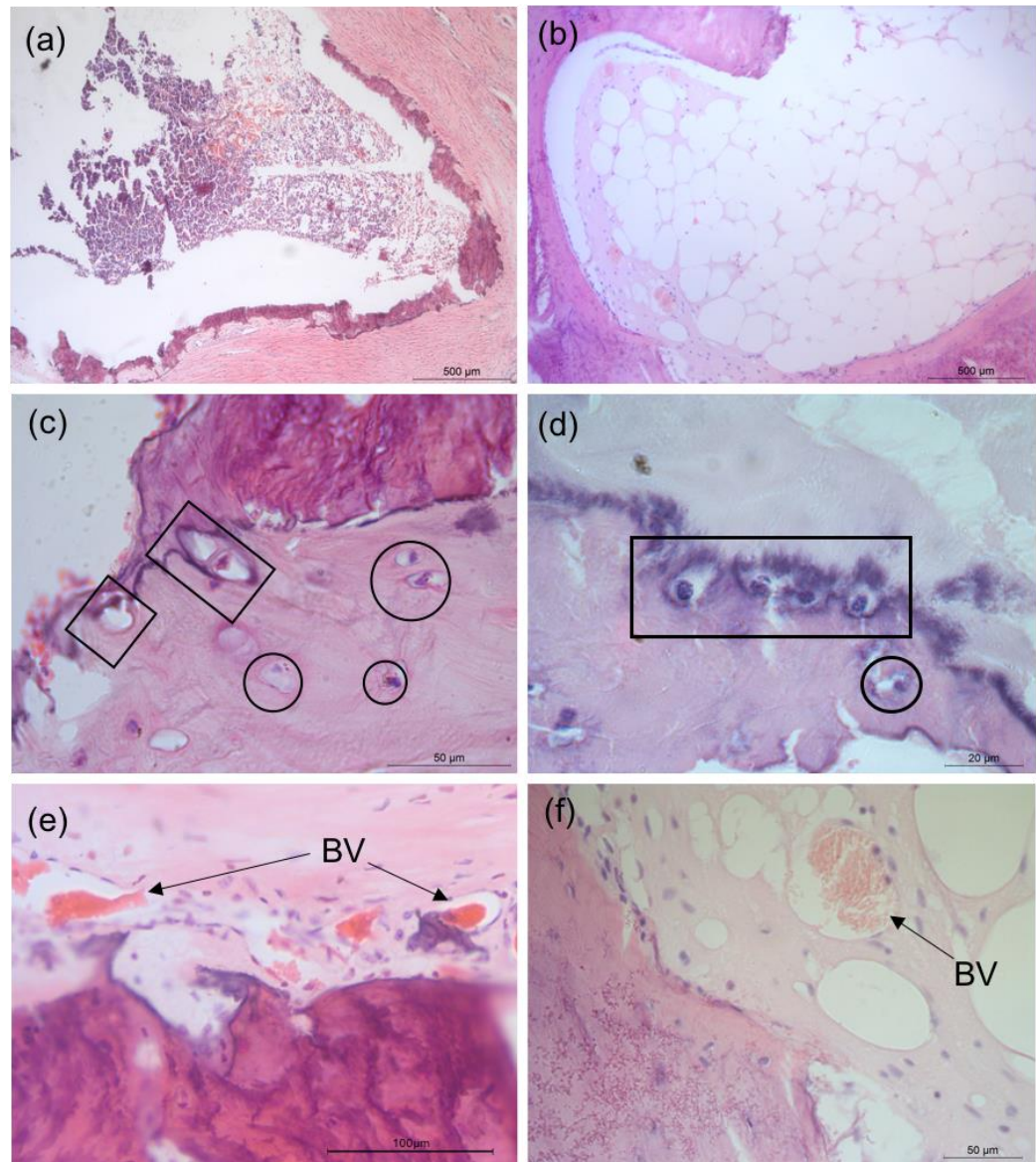
Figure. 4.5. Photomicrographs of nyala and giraffe os cordis stained with H+E demonstrating evidence of bone tissue, cartilage tissue and endochondral ossification. (a) Nyala (Sample 1), bone with internal marrow of haematopoetic cells. (b) Giraffe (Sample C), bone with adipose marrow. (c,d) Nyala (Sample 2) and giraffe (Sample B), evidence of endochondral ossification as chondrocytes invade bone indicated in boxes and chondrocytes within ectopic cartilage indicated by circles. (e,f) Nyala (Sample 5) and giraffe (Sample C) showing blood vessels (BV). Scale bars represent 500µm (a+b), 100µm (c) and 50µm (d).

4.3.5. Special Stain Histological Analysis of Hyperdense Structures in Nyala and Giraffe.

To further confirm the presence of bone, and in some cases cartilage, special stains were performed. The use of picrosirius red stains (ab150681, Abcam, UK) allowed for visual and computerised analysis of collagen types within each heart. Microscopic observations showed increased levels of thicker red fibers (likely type I collagen) occurred around the periphery of bone and cartilage tissue (Figure. 4.6a+b). Computerised techniques were then used to identify the exact ratios of each collagen type using colour recognition. Ratios of thick red fibers were compared to finer green fibers (likely type III), these ratios remained consistent between both species in the samples where bone was present with 16% red fibers. However, in the myocardium where bone was not present the percentage of red fibers in the giraffe rose to 42% and in the nyala fell to 11% of the collagen fibres present (Figure. 4.6h). Von Kossa (HC9913161, Merck Millipore, Germany) stained positively in both the nyala and giraffe indicating that calcium deposits were present, indicative of bone (Meloan & Puchtler, 1985; Figure. 4.6c+d). Immunohistochemistry (7150-K, Leica Biosystems, Germany) of nyala samples merited one immunopositive cell, indicating the presence of ALPL in an osteoblast, while no such cells were found in the giraffe (Rutland et al. 2021; Figure. 4.6g). Alcian blue (J60122, Alfa Aesar, USA) staining at pH 0.2 stained a deep blue colour around cartilage and could also be seen in lighter shades in the bone tissue and myocardium (Figure. 4.6e+f). This suggested presence of acid mucins, notably glycosaminoglycans which are usually present in cartilage.
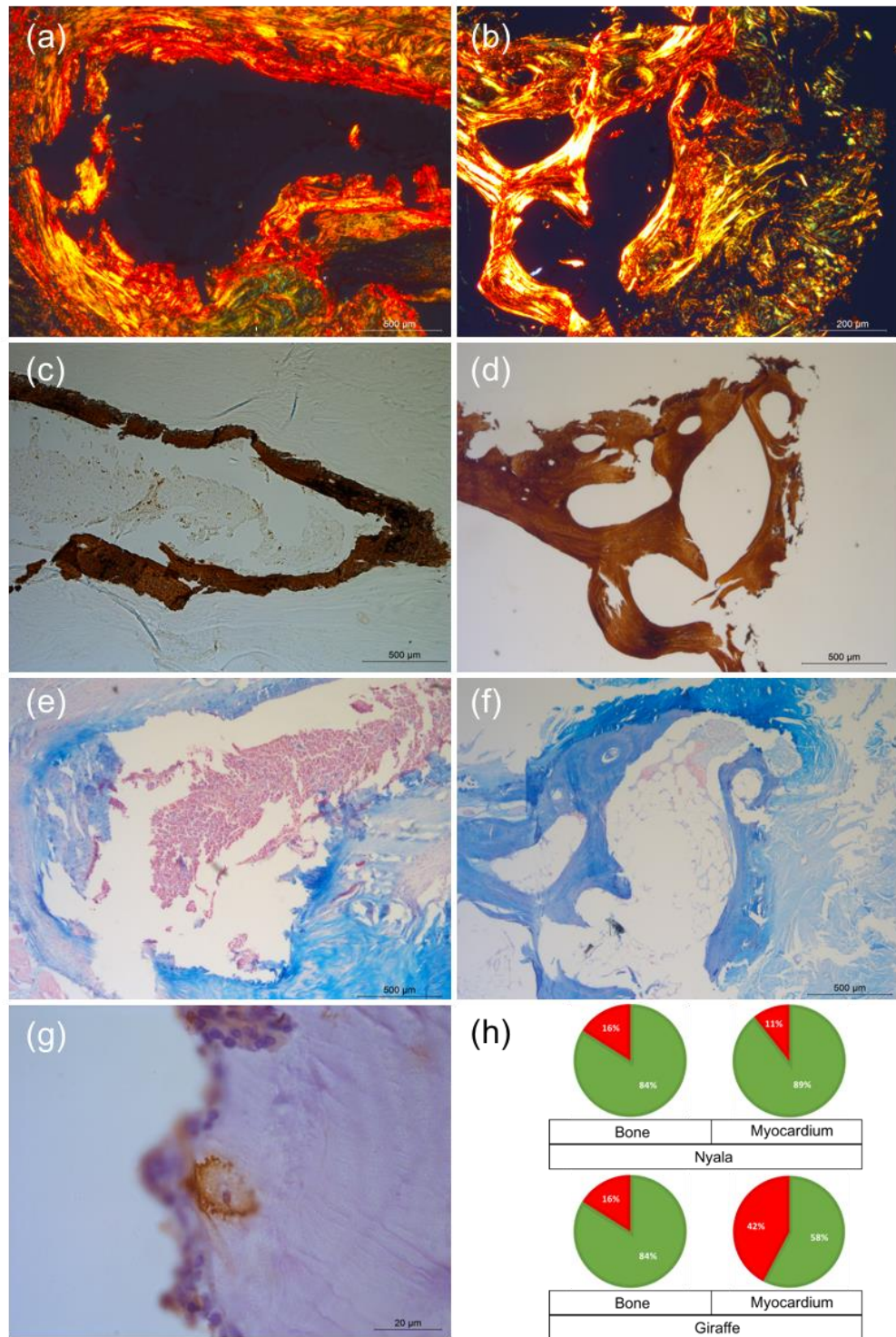
Figure. 4.6. Nyala (left) and giraffe (right) heart tissue stained with various special stains, gathering further evidence to observations made with H+E. Alongside a pie chart showing percentages of red (likely collagen type I) vs green fibers (likely collagen type III) in heart tissue samples from nyala and giraffe, containing bone or no bone (h). (a-b) Nyala Sample 6 and giraffe Sample B stained with picrosirius red. (c-d) Nyala Sample 6 and giraffe Sample B stained with Von Kossa. (e-f) Nyala Sample 6 and giraffe Sample B stained with alcian blue at pH 0.2. (g) Positively stained nyala cell by immunohistochemistry within the Sample 6. Scale bars represent 500µm (a, c, d, e + f), 200µm (b) and 20µm (g).

4.4 Discussion

The aim of this study was to investigate a nyala and a giraffe heart for hyperdense tissue, whether that would be cartilage (cartilago cordis) or bone (os cordis). By using microCT alongside histological techniques it was possible to show that a single os cordis was present in the giraffe heart within the interatrial septum. Additionally, in the nyala, a unique finding of four cardiac bones was discovered. One bone was found at the base of the aorta, one in the wall of the right atria and two bones were found in the regions of the interatrial and interventricular septa. This is the first discovery of any ossa cordis in the nyala and is the first report of giraffe os cordis being investigated using radiographical and histological techniques with detailed morphological and histological details revealed. Alongside the discovery of os(sa) cordis, this study also showed the novel discovery of cartilage tissue within both hearts, and showed evidence of how that cartilage indicates ossa cordis development via EO. These discoveries, alongside a systematic review of the published literature, shows the occurrence of os(sa) cordis in even more *Artiodactyla* species and could suggest that similar investigations into other species, particularly those from the *Artiodactyla* order, may merit similar investigations.

No abnormalities were detected in the cardiovascular systems of either of the nyala or giraffe during preliminary investigations by a veterinary pathologist. Therefore, it is unlikely that bone formation was impacted by disease influence therefore, the ossa cordis found in these hearts are likely to be an anatomically normal finding. However, investigations into more giraffe and nyala hearts should be completed in addition to the single hearts from this study to confirm this. Historically, it has been shown that bone formation can result from CVD conditions, namely ischemia (Lehoczky-mona & McCandles, 1964). Subsequently, the discovery of os(sa) cordis in some species has been attributed to CVD (Moittie et al. 2020; James & Drake, 1968). CVD evidence was found during later histological investigations in the nyala heart however, this finding on its own does not imply disease involvement, investigation of multiple additional nyala hearts is required to look whether CVD influences os(sa) cordis formation in this species. The investigation of the giraffe heart provides additional evidence that os cordis development does occur, at least in some cases, in giraffes without obvious CVD influence, as the heart appeared healthy in preliminary and histological investigations.

The nyala OCD and the singular giraffe os cordis both showed chondrocytes undergoing EO, a process which has been extensively discussed in the published literature. Previous studies in the water buffalo, camel, horse, sheep and chimpanzee have eluded to EO as a possible route for os cordis development due to observations of cartilage in close proximity to bone, or by observing cartilage in younger individuals in the same region as future developed os cordis in older hearts (Daghash & Farghali, 2017; Ghonimi et al. 2014; Matsuda et al. 2010; Gopalakrishnan, 2007; Moittie et al. 2020). In addition, similar to findings in the nyala and giraffe, a number of otter hearts showed direct histological evidence of EO (Ergerbacher, 2000). These observations can therefore add supporting evidence to the hypothesis that

os(sa) cordis develop form cartilage by EO, as cartilage was observed in close proximity to bone and chondrocytes were observed invading into bone tissue in present studies.

The presence of thicker, picrosirius red stained collagen fibers (likely type I collagen) around the periphery of bone in the nyala provides further evidence towards the theory of EO. Chondrogenesis and osteogenesis in normal neonatal development throughout the body requires constant involvement of type I collagen, hence prechondroblasts contain the mRNA required to produce type I collagen (Wulf et al. 1994). This type I collagen is then replaced by type II collagen during cartilage development and when the cartilage is subsequently ossified type I collagen is detectable again in ossifying chondrocytes (Dessau et al. 1980; Wulf et al. 1994). In the giraffe myocardial samples in the present study, the percentage of red (presumed type I collagen) fibers was vastly larger than that quantified in the nyala. It is not known why this occurred but one theory is that the giraffe heart contained more red (likely type I) fibers because the bone in this heart was still developing via EO and so required constant involvement of type I collagen whereas the nyala heart had a lower proportion of these fibers which may indicate that the ossa cordis were fully developed. However, this finding only occurs in regions of the heart further away from the bone and does not explain why collagen proportions immediately adjacent to each os(sa) cordis were so similar. Naturally species differences could be naturally present, or indeed individual ages differences may also help explain the differing levels of type I collagen. Both the nyala and giraffe were adult at time of death. The giraffe was 11 years old and approximately 44% through its average lifespan whereas, the nyala was 5 years old and approximately 27% through its average lifespan (Maisano, 2006; Ciszek, 1999). This suggests that if the giraffe os cordis was still in development at the time of this study, as the PSR analysis indicated, the os cordis in the giraffe could develop later on in life compared to the nyala. This later development would contrast to most other mammalian species with os(sa) cordis, for example in the water buffalo os cordis has been found in individuals from 3 years of age, approximately 9% through their average lifespan (Roth, 2004).

In chimpanzees it was suggested that os cordis formation could have been attributed to HO, the formation of bone within soft tissue (Moittie et al. 2020; Kaplan et al. 2004). Collagen patterns between HO and EO are in principle similar however, HO is also critically linked with factors such as an inflammatory response and hypoxia, associated with CVD, which was also present in some of the chimpanzees investigated (Wulf et al. 1994; Ranganathan et al. 2015; Moittie et al. 2020). Therefore, EO should be considered as the principle theory towards the formation of os(sa) cordis in cases without CVD though, HO is still possible. Further investigation into the factors involved in HO and EO bone development in these species could allow us to see more clearly what process or processes manufactures os cordis, by identifying which factors are expressed during os cordis development.

Similar to some mammals which have os(sa) cordis, two of the four nyala ossa cordis (os cordis intermedius and inferior sinistrum) and the single giraffe os cordis were found in the anatomical regions of the interatrial and interventricular septa. The locations of these bones in this region which is subject to such high mechanical stress may suggest that the function of these bones is to help protect the heart from shearing under these forces. Also residing in this region are the major conductive heart cells and tissues, and therefore it could be suggested that the bones are present to prevent damage to these critical conductive tissues. This hypothesis has been suggested in other species with os(sa) cordis which reside in similar locations (James, 1965; Frink & Merrick, 1974; Ergerbacher et al. 2000). The two other ossa cordis in the nyala share few similarities to other species. Os cordis superior sinistrum, present at the base of the aorta, is comparable to the most cranial part of the OCD in cattle and camels however, the presence of a whole bone residing in this region has only previously been seen in a similar species to nyala, the white-tailed deer (James, 1965; Ghonimi et al. 2014; Rumph, 1975). The most peculiarly positioned bone in the nyala is the largest, OCD, positioned within the wall of the atria on the right side of the heart. The only comparison which can be made to this is the discovery of a third bone in sheep residing in the right atrial wall however, the bone was considerably smaller than that found in the nyala and, in fact may be a fragment of OCD since only the right atria were investigated in the study (Gopalakrishnan, 2007). It is difficult to explain why these bones developed in these areas and there is no clear evidence towards their function. OCD occurs in the wall of the right atrium, where the sino-atrial node also resides and so the hypothesis that os(sa) cordis works to protect conductive structures such as this would match the bones position, but this theory does not suggest a reason for the sheer size of the bone, spanning nearly the whole length of the atria some of the ventricle. Os cordis superior sinistrum resides in an area which is similar to that of the human fulcrum, a structure which has been shown to aid in the coordination of heart contractions acting as an anchor for myocardium insert into and contract against (Trainini et al. 2020). Therefore, the os cordis superior sinistrum could act in a similar way to aid contraction in the nyala. The human fulcrum demonstrates another way in which hearts can adapt to overcome high mechanical forces without, in most cases, developing an os cordis. Further anatomical studies should be performed investigating more species to see if tougher tissue types develop in hearts with high mechanical pressures, how and when these tissues develop and why they develop instead of os(sa) cordis.

Despite only investigating one heart for both the nyala and giraffe, the findings in this study can confirm the novel discovery of four ossa cordis in the nyala and provide a more detailed exploration of the giraffe os cordis. In addition, it is likely that similar findings would be apparent in other individuals from these species as neither of the animals investigated in this study had a severe degree of CVD. This could suggest that the os(sa) cordis seen in this study occurred as a natural event. However, in order to confirm os(sa) cordis as a natural event in each of these species many more hearts from both species should be analysed in the future. By investigating hearts of varying ages and disease states it would be possible to show whether this discovery is an anatomically normal event or whether it is prompted by factors

such as pathological cardiac conditions or natural aging. Additionally, further investigation may show when os(sa) cordis develops and if they are pertained by cartilage, solidifying claims of EO.

Aside from the obvious advantages this research possesses towards improving the understanding of cardiac anatomy in these two species, this study also introduces some interesting factors regarding the presence, or lack of, os cordis in different species within the *Artiodactyla* order. The discovery of os(sa) cordis in these two species, alongside previous findings in cattle, sheep, goat, water buffalo, deer and camels demonstrates that cardiac bone is a common finding in the *Artiodactyla* order. This poses the question that if more species were investigated in a similar manner to this study, would more novel discoveries of os(sa) cordis in differing species be made? Being able to investigate and discover more species with os(sa) cordis would not only provide more knowledge on the formation, function and presentation of os(sa) cordis within the *Artiodactyla* order but, in fact, could help us to understand why and how os(sa) cordis develops in species outside of this order and why this formation is often associated with CVD. When os cordis has developed in the heart with association with CVD it has been shown that the formation of bone has contributed towards an increasing severity of pathological cardiac symptoms including sudden death (Ferris & Aherne, 1971; Moittie et al. 2020; James & Drake, 1968; Liu et al. 1975). Therefore, investigating the factors involved in the formation of os(sa) cordis as a physiologically normal event and as an event associated with CVD would allow us to observe the differences/similarities between these two events. Investigating these factors could allow us to predict when and why os(sa) cordis forms in all species. This could help in the treatment and control of certain CVDs in cases where bone forms as a result of disease. It is not known whether ossa cordis escalates or alleviates the progression of disease, treatments targeted towards preventing/reducing the process of bone development if necessary therefore improving prognosis, or understanding the mechanisms employed to understand the requirements of the heart. Increasingly, surgery is being used to alleviate cardiovascular problems, if ossa cordis help alleviate cardiovascular abnormalities it would be worth investigating whether mimicking them surgically/with implants prove effective. Pharmacological interventions using gene and cell mechanism pathways be a route to alleviating heart disease and treating cardiovascular abnormalities.

5. Investigation of the Cardiac Skeleton in Two Great Apes, the bonobo and Gorilla, with reference to the Presence of Hyperdense Tissues.

This chapter demonstrates the novel investigation of 15 Gorilla and nine bonobo hearts for hyperdense tissues. An investigation into the cardiac anatomy of a chimpanzee in 2020 merited the novel discovery of os cordis, a hyperdense structure in the heart. Subsequent evidence from this study suggested the instance of os cordis had a positive correlation with fibrosis, specifically from CVD such as IMF (Moittie et al. 2020). In response to these findings, further studies into the Gorilla and bonobo sought to investigate whether these discoveries were consistent in more captive great ape species. It explored the question as to whether the Gorilla and bonobo also develop hyperdense cardiac structures, and if they were present was their presence/formation linked to fibrosis?

5.1. Rationale, Aims, Objectives and Hypothesis

Investigating the Gorilla and bonobo using microCT, dissection and histology will allow for greater understanding of the cardiac anatomy within these species. The specific investigation of hyperdense structures using these techniques enabled the first investigation into the hyperdense structures and also enabled a comparison of Gorillas and bonobos with other species which have been shown to present with hyperdense cardiac structures, in particular the chimpanzee. By assessing the existence/incidence of hyperdense structures within ape hearts alongside assessments of each hearts fibrosis level, the relationships between fibrosis and the formation of hyperdense tissues, not only in captive apes, but in other mammalian species, could be understood.

To ascertain whether hyperdense structures occurred in Gorillas and bonobos, and whether they occur in parallel with increasing severity of fibrosis, extensive macroscopic investigations of each heart were used to determine the fibrosis level within each specimen. This was followed by further dissection, microCT scanning, histology and microscopy of the cardiac tissue and any hyperdense structures.

It was hypothesised that all Gorilla and bonobo hearts would present with varying levels of fibrosis and that the levels of fibrosis may increase with age. It was also hypothesised that increased levels of fibrosis would result in a positive association with cardiac hyperdense structures (such as os cordis or cartilago cordis).

5.2. Introduction

CVD contributes to a large proportion of mortalities in great apes in captivity. From 1990 to 2003, as many as 77% of captive great apes were reported to have CVD at time of death (Gamble, 2004). The most common CVD is IMF, an accumulation of fibrous tissue within the heart, which results in impaired cardiac function and in some cases, sudden death (Strong et al. 2020).

A study which first identified os cordis in the chimpanzee found that its occurrence was related to increasing fibrosis levels (Moittie et al. 2020). The study identified three chimpanzee hearts which contained bone (os cordis) and one further heart which contained cartilage (cartilago cordis). Each of these hearts was determined as at least fibrosis level five out of six, and statistical analysis confirmed that those hearts presenting with cartilage or bone (cartilago cordis or os cordis) had significantly higher levels of fibrosis in comparison to hearts without these structures.

No previous studies have investigated Gorillas or bonobos for presence of hyperdense cardiac structures, and since the Gorillas and bonobos included in the present study were all kept in captivity it is likely that these individuals would present with IMF. Therefore, it is possible that similar to the chimpanzee, high fibrosis levels from IMF could result in the novel discovery of bone, cartilage or other hyperdense tissues in the hearts of these closely related great apes.

5.3. Results

5.3.1. Initial Macroscopic Examination and Histology

As an essential part of these investigations all hearts were investigated by a certified veterinary pathologist. These described fibrosis levels within each heart including both interstitial fibrosis and replacement fibrosis. All 24 hearts were subsequently assigned a fibrosis level from 1-5 based on the following comments: Level 1, none to minimal fibrosis; level 2, minimal to mild fibrosis; level 3, mild fibrosis; level 4 moderate fibrosis and level 5, moderate to extensive fibrosis (Table. 5.1). Analysis undertaken in this project showed that although the average age of individuals in level 1 were lower than in all other levels for both Gorilla and bonobo. (Table. 5.1).

Fibrosis Level	Description	Gorilla (ID Number)	bonobo (ID Number)	Average Age (yrs)	
				G	B
1	None - Minimal	12, 7, 9	8, 4, 2, 3	5.6	12.3
2	Minimal – Mild	3, 13, 15, 16, 17	-	42.7	-
3	Mild	10, 2, 4	5, 6	51.8	30.0
4	Moderate	6, 11, 1	-	31.8	-
5	Moderate - Extensive	8	1, 7, 9	41.3	19.7

Table. 5.1. Fibrosis levels of each Gorilla and bonobo heart investigated. The description of each fibrosis level given by a veterinary pathologist, and the average age of each fibrosis level for both Gorilla (G) and bonobo (B).

None of the individuals in the highest fibrosis level from either species contained hyperdense structures. One of the hyperdense structures that was found belonged to an individual (G3) from the second lowest fibrosis level (level 2), whilst the remaining individual with hyperdense material was level 4 out of 5. This suggests that in this study no correlation could be found between occurrence of hyperdense tissues and level of fibrosis. Naturally with such low levels of animals showing hyperdense materials from this cohort (15 Gorillas and 9 bonobo), it was not possible to undertake detailed statistics or correlations, a higher number of individuals with significant hyperdense cardiac structures would be required.

Statistical analysis was run on between the ages, fibrosis levels of bonobo and Gorilla hearts. ANOVA with Bonferroni Post Hoc tests were run to ascertain if there was a link between age and the fibrosis level given to each heart. For Gorilla hearts, fibrosis levels 4 and 5 were grouped together prior to the test being run due to only one Gorilla heart being placed in level 5. The result of the test showed there was no significant association between fibrosis levels and age with a P-value of 0.064. Additionally, the same test was run comparing groups 1 and 2 with groups 3, 4 and 5, again no significant association was found with a P-value of 0.926. Regarding bonobo hearts, there was again no significant association between ages and fibrosis levels of the hearts. This shows that in the sample there was no evidence that age effected levels of fibrosis in the heart despite a small positive correlation between average age and fibrosis level in Gorilla hearts (Figure. 5.1)
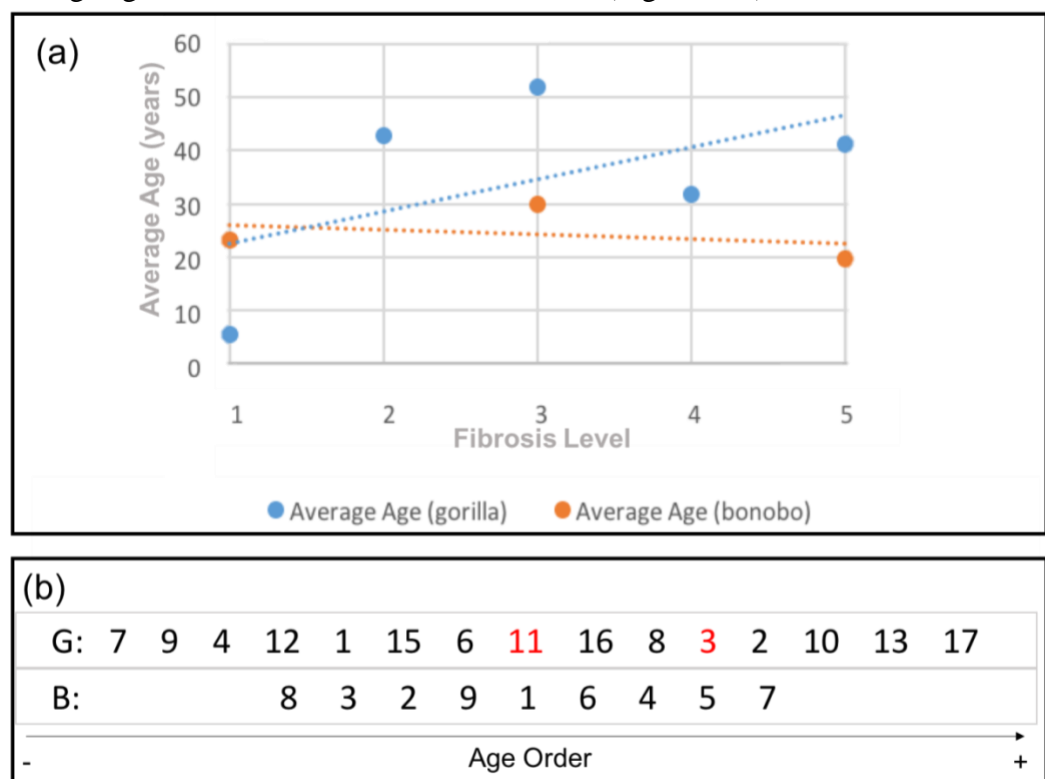
Figure. 5.1. A graph showing the average ages of Gorillas and bonobos within each fibrosis level (a) Above an ordered list of the Gorilla (G) and bonobo (B) hearts investigated in this study from youngest to oldest (b). Highlighted in red are the individuals where hyperdense structures were found.

5.3.2. X-ray Computed Microtomography

In order to identify all hyperdense tissues within the Gorilla and bonobo hearts, microCT was performed on each heart. Throughout all of the hearts, multiple very small hyperdense structures were visible (Figure. 5.2b), however, these were not thought to be significant features (small plaques or background noise from scanning) and so were not investigated further. In total 20 ROI (from 12 Gorilla + 8 bonobo hearts) were identified from microCT as having significant hyperdense structures, therefore these underwent further investigation using dissection and histology (Table. Appendix. 2). As mentioned in Section 2.3, representative samples from other hearts (not containing hyperdense structures) were also investigated for the regions similar to the 20 ROI, ensuring that all 15 Gorilla and nine bonobo hearts were investigated, in addition to control tissues. The most noteworthy of the 20 regions (found in Gorilla 11; G11) contained a cluster of joined hyperdense structures within aortic tissue near the aorta's origin from the heart (Figure. 5.2a, c). These structures, when considered as a single structure measured 3.4mm in length, 0.4mm width and 0.3mm depth. MicroCT showed that the structure consisted of a hyperdense shell with a less dense interior, it showed no characteristics of bone, such as trabeculation. In addition to the images given below, a further seven microCT scans of Gorilla hearts are provided in Appendix. 1
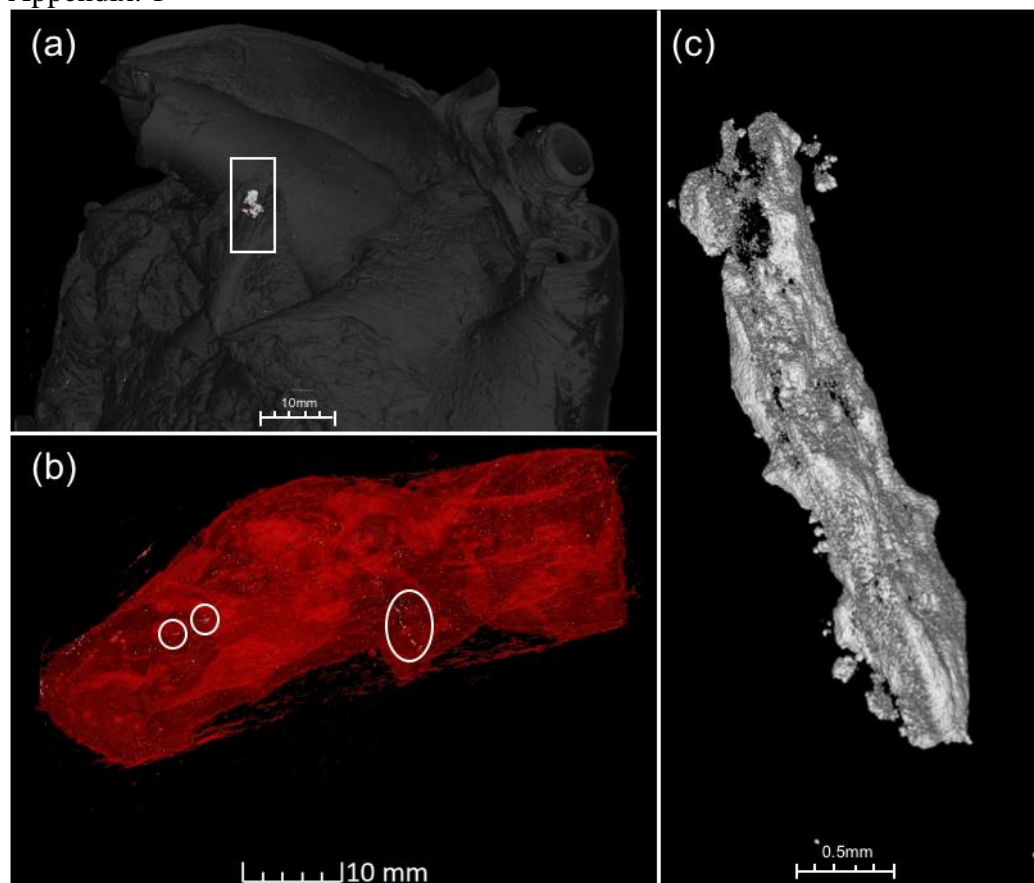
Figure. 5.2. MicroCT scans of Gorilla (a, c) and bonobo (b) hearts. The box in (a) indicates the notable structure found in G11. Circles in (b) indicate examples of the small hyperdense structures seen in all hearts. (c) Represents a higher definition image of the structure shown in the box in (a). Scale bars represent 10mm (a, b) and 0.5mm (c).

5.3.3. Histology of Great Ape Heart Tissue

In all of the hearts cardiomyocytes were seen and formed in a typical striated pattern within the myocardium. Blood vessels were also observed within the myocardium, these contained erythrocytes (Figure. 5.3a+b). In two of the Gorilla and in five bonobo hearts, the myocardium presented with a waved pattern, indicative of plexiform fibrosis (Figure. 5.3c). Additionally, an abnormal number of adipocytes and 'free' erythrocytes were observed within the myocardium tissue in eight Gorilla and three bonobo hearts (Figure. 5.3d).
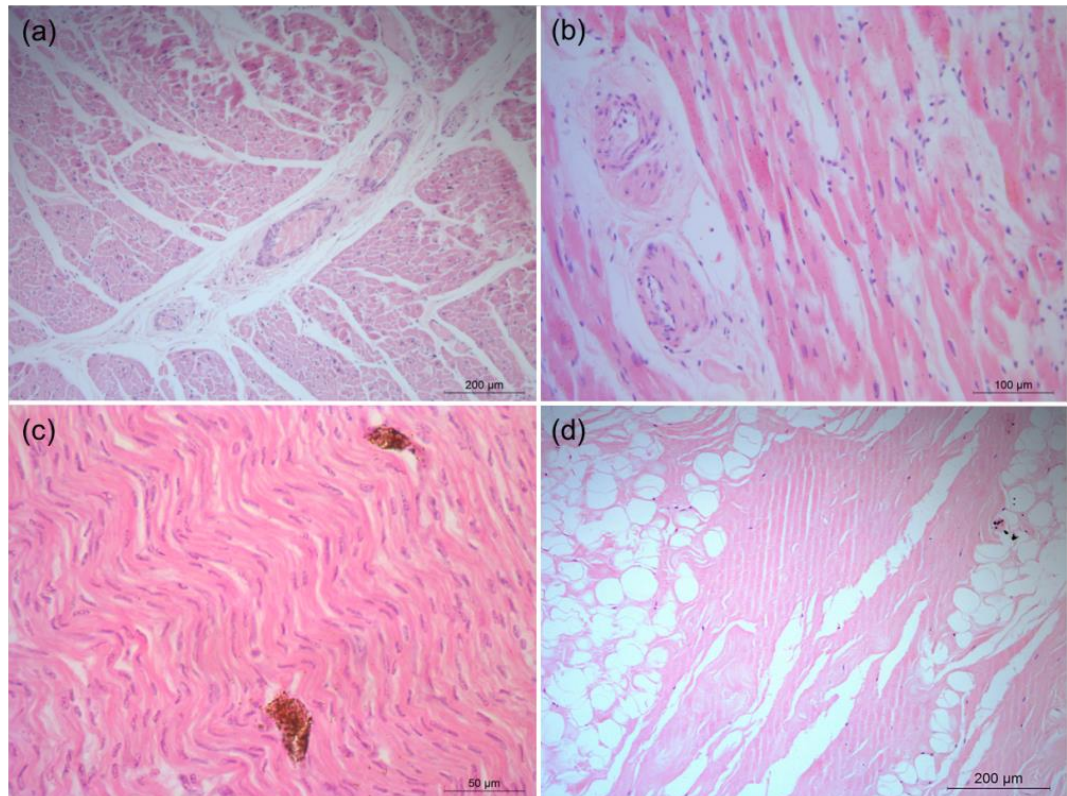
Figure. 5.3. Photomicrographs of bonobo and Gorilla myocardium stained with H+E demonstrating the morphological effects of cardiovascular disease. bonobo (a) and Gorilla (b) samples demonstrating healthy tissue with vessels. bonobo (c) and Gorilla (d) tissue demonstrating abnormalities observed such as wavy tissue and a high numbers of adipocytes. Scale bars represent 200µm (a+d), 100µm (b) and 50µm (c).

5.3.4. Histology of Hyperdense Tissue found in the Primate Heart

The structure found in G11 during the microCT scanning was observed using histological techniques including H+E staining. The structure consisted of a dense cortical layer and homogenous internal matrix, and was therefore suspected to be a dystrophic plaque (Figure. 5.4a, c). In addition to the G11 sample, a smaller hyperdense structure was detected within H+E stained tissue (and on microCT) from Gorilla 3 (G3). This structure was smaller and morphologically resembled bone (Figure. 5.4b, d), however no osteocytes, osteoblasts or osteoclasts were detected within the H+E stained tissue from G3, therefore the structure could not be confirmed as bone. The structure, which was highlighted as a region of interest after microCT measured 2mm in length, 0.7mm in width and 0.4mm in depth. No hyperdense tissues were detected using histology from any of the remaining 20 ROI or any of the control representative samples taken from the other hearts, which included all of the bonobo hearts.
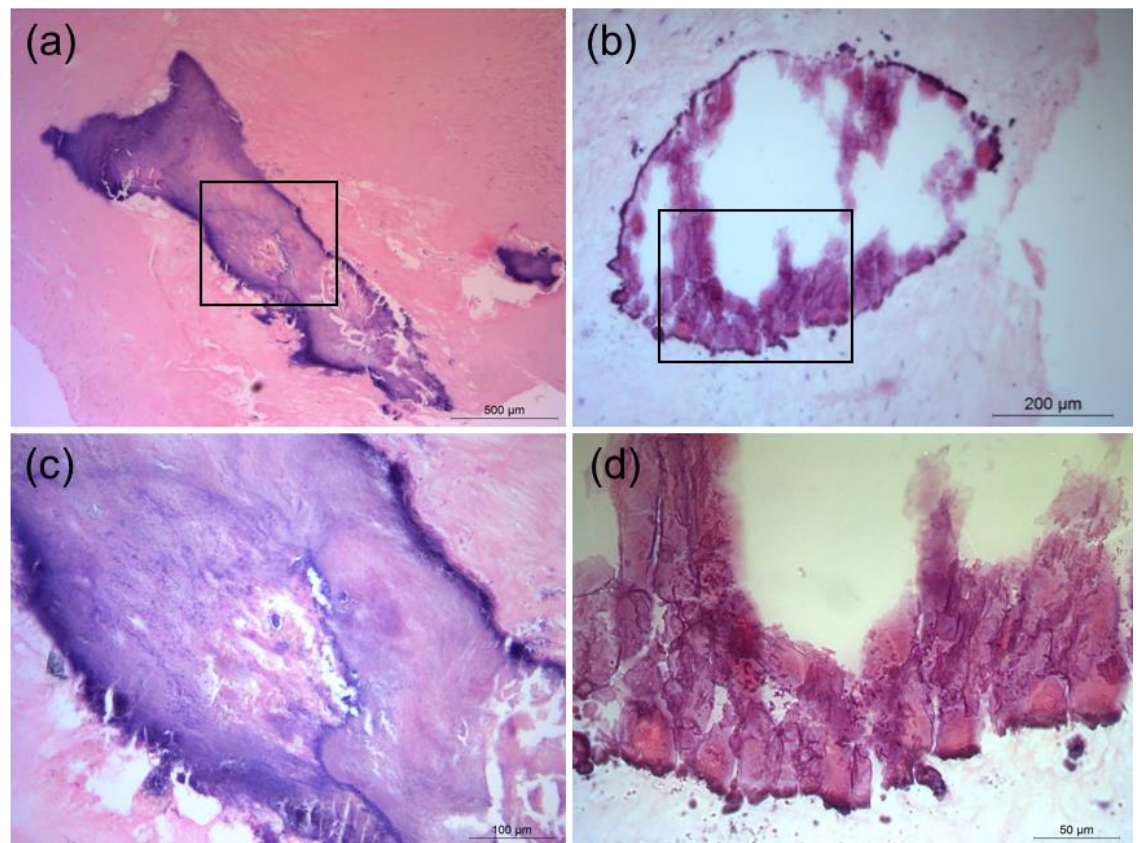
Figure. 5.4. Photomicrographs of hyperdense structures in Gorillas using H+E staining showing morphological evidence of hyperdense plaques. A suspected dystrophic plaque in G11 (a), and a hyperdense structure from G3 (b). (c, d) Corresponding magnified images of (a) and (b) respectively. Scale bars represent 500µm (a), 200µm (b), 100µm (c) and 50µm (d).

In order to define the tissue types within each structure, Von kossa, alcian blue, PSR and immunohistochemistry stains were performed. The structure in

G11 stained positive for calcium (using Von kossa staining) within the hyperdense structure providing more evidence that this structure was a calcified dystrophic plaque (Figure. 5.5a). The hyperdense structure in specimen G3 also stained positively for calcium by Von kossa stain (Figure. 5.5b). Neither of the hyperdense structures from specimens G3 and G11 showed positive staining when exposed to ALPL antibodies during immunohistochemistry. It was determined that either no osteoblasts were present to stain or that the immunohistochemistry protocols/antibodies did not work on this tissue. Both hyperdense structures from the two Gorilla specimens stained with PSR showing the varying collagen types in each structure (Figure. 5.5e+f). The staining in each specimen was similar when compared to each other, and although collagen types I and III and undifferentiated collagen were present, no evidence of cartilage was observed in either sample. Despite the lack of cartilage in the sample, positive AB staining still occurred due to a presence of acidic polysaccharides.

Following PSR staining, computerised analysis was performed on photomicrographs of PSR stained tissue from both species. Analysis showed that finer green fibers (most likely type III collagen) were more abundant than thicker red fibers (most likely type I collagen) in all samples. No bonobo samples contained any evidence of hyperdense structures. The bonobo samples stained with PSR presented with 34% red fibers and 66% green fibers on average (Figure. Appendix. 3). The Gorilla samples without hyperdense structures had a higher proportion of red fibers at 40% (60% green fibers) than Gorilla samples with hyperdense tissues present which contained 36% red fibers (64% green fibers; Figure. Appendix. 3).
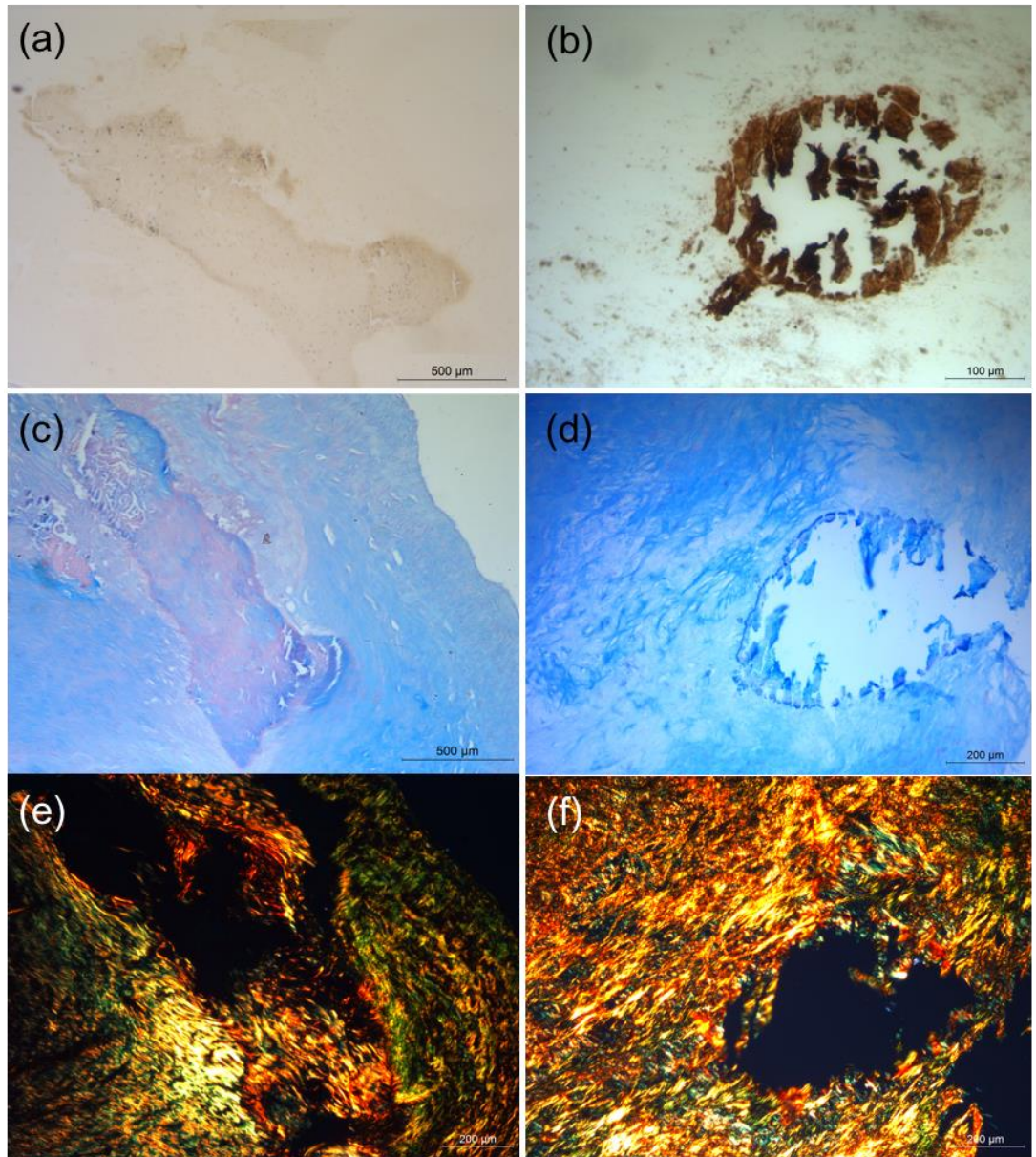
Figure. 5.5. Representative photomicrographs of Gorilla hyperdense structures exposed to differing special stains. Samples G11 (a, c+e) and G3 (b, d+f), stained with Von kossa showing calcium in tissues (a, b), alcian blue to identify cartilage if present (c, d), and picrosirius red to help identify collagen types I (red), III (green) and undifferentiated collagen (e+f). Scale bars represent 500µm (a+c), 100µm (b) and 200µm (d, e+f).

5.4. Discussion

Studies using human and animal models have shown that increased levels of collagen deposition in the heart increased with age causing greater levels of cardiac fibrosis (Mukherjee & Sen, 1990; Song et al. 1999). By looking at the ages of individuals from this investigation one can see that from fibrosis levels one to three, the average age of the individuals in each level increased. However, from levels three to five the average age of fibrosis levels did not increase with fibrosis (Figure. 5.1). Despite this trend it was shown during ANOVA Post Hoc tests with Bonferroni that there was no significant association between age and fibrosis level. This was thought to be because hearts selected for investigation were not selected at random but instead chosen to represent similar ages within different fibrosis levels to see if age/ fibrosis was a factor in occurrence of hyperdense structures. Additionally, it is likely that the occurrence of CVD, namely IMF in this case, skews this correlation between age and fibrosis. For example, high degrees of myocardial fibrosis from IMF in younger individuals may be comparable to older individuals with low to no levels of IMF but similar fibrosis levels on the whole due to increasing collagen deposition with age. Therefore, when considering the fibrosis level of an individual and how it may correlate to the presence/lack of hyperdense cardiac tissues, the age of the animal must also be considered alongside its given fibrosis level as a different and potentially complicating factor. For example, the two animals which presented with hyperdense tissues in this study were G3 and G11. G3 belonged to fibrosis level 2, and was the 4th oldest of the Gorillas studied (43yrs), while G11 was a fibrosis level 4 and was only the 9th oldest of Gorillas studied (34yrs, see Table. 5.1). Therefore, the fibrosis in G3 could be largely attributed to age whereas the fibrosis seen in G11 is more likely to be predominately a result of disease. In mammals other than the chimpanzee, os(sa) cordis has been shown to occur more often in older individuals, therefore it is also highly likely that os(sa) cordis occurrence is linked to higher levels of fibrosis (Ergerbacher et al. 2000; James & Drake, 1968; Daghash & Farghali, 2017; Endo et al. 2005). Additionally, os cordis formation has been proven to have a positive correlation with higher levels of IMF in chimpanzees regardless of age, again suggesting that os cordis instance occurs in parallel with fibrosis (Moittie et al. 2020). Contrasting this was the findings found in this study, where the hyperdense structures did not follow this pattern. The instances of hyperdense structures found in this study belonged to G3 which had a fibrosis level of 2 out of 5 and G11 which did have a high fibrosis level of 4 out of 5, yet other higher level fibrosis individuals did not have bone or cartilage hyperdense material in the heart.

Since only two hyperdense structures were identified in this study it is not possible to confirm that the occurrence of these structures had no correlation to severity of disease and/or fibrosis level. It was also difficult to suggest whether there were any similarities between the hyperdense structures found in this study and os(sa) cordis/cartilago cordis found in other mammals. Further investigation of dystrophic plaque formation in great apes on a greater scale could allow us to assess the relationship between plaques and fibrosis level (whether that be age or disease related). These trends could be assessed

and compared with ossa cordis occurrence to examine potential links between dystrophic plaque formation in the heart and os(sa) cordis formation.

The most distinct limitation to the investigation of these two great apes was the process of identifying and collecting ROI from each heart. MicroCT scanning showed numerous minor hyperdense structures as well as 20 ROI which were selected for sample collection. Since each heart had already been through post mortem and preliminary macroscopic investigations, by the time sample collection via dissection was performed it was very difficult to ascertain the exact location of each ROI. Each heart was positioned carefully for microCT and secured using polyethylene wrap. Once this wrap was removed for sample collection the position and shape of the heart altered, making it difficult to locate the exact position of each ROI originally identified on microCT scans. Only two out of 20 ROI merited hyperdense tissue from histological investigations. It is therefore possible that any of the remaining 20 regions which showed hyperdense tissues on microCT scans also contained hyperdense structures which have not yet been investigated fully via histological methods. Not only that but numerous minor structures were seen on microCT which were categorised as insignificant, and therefore were not investigated. These minor structures were excluded as they could have been debris within the sample, or an artefact from scattered x-rays, and so it was unlikely, although possible, that these minor structures were plaques, bone or cartilage. Further investigation into these minor structures could have merited the discovery of more hyperdense tissues in more hearts.

The hyperdense tissue found in G11 could be confirmed as a dystrophic plaque by its morphological appearance when stained with H+E and was located within aortic tissue close to where the aorta originates. Previously, os cordis has been found in this region of the heart, although affiliated with myocardial tissue at the base of the aorta rather than being within aortic tissue itself. Os cordis in the white-tailed deer is also present at the base of the aorta and the cranial part of OCD in cattle and camels (Pour, 2004; Ghonimi et al. 2014). Additionally, os cordis superior sinistrum, discovered as part of this thesis in the nyala, was also found at the base of the aorta, again surrounded by myocardial tissue rather than aortic tissue. It is therefore possible that the formation of hyperdense tissue has some affiliation to this region, although the exact reason for this is unknown. The region is prone to high mechanical forces as blood is expelled from the aorta and so the theory that hyperdense tissues could work to protect tissues from shearing under these forces could be applied. This theory has been used to explain why os(sa) cordis develop within the regions of the major cardiac septa in other species (Frink & Merrick, 1974; Mohammadpour & Arabi, 2007; Pour, 2004; Ghonimi et al. 2014). However, currently it is not possible to know if this theory applies to plaques and os(sa) cordis tissue, and since the exact process by which this plaque formed is unknown and it cannot be presumed that the plaque formed in this region in response to high mechanical forces, such as been suggested in instance of os(sa) cordis. Further research into how dystrophic plaques form within the heart and what factors trigger this formation could allow us to predict whether the formation of these plaques occurs in this region due to similar reasons hypothesised for os cordis or for other reasons.

The hyperdense structure found in G3 was located within the interatrial septa, a region where os cordis is commonly found in some other mammals (Frink & Merrick, 1974; Mohammadpour & Arabi, 2007). Although comparative to os cordis in its location, the hyperdense tissue found in G3 could not be confirmed as bone. The morphology of the structure was similar to bone however no cells were observed within bone from H+E stained slides nor from immunohistochemistry. The interatrial septum, similar to the base of the aorta, is exposed to high mechanical forces during cardiac contraction and so the development of hyperdense tissue in this region in the Gorilla could be affiliated to this. More research is required to firstly ascertain whether similar structures appear consistently in Gorilla hearts and secondly, and what the exact cellular and molecular structures and composition of these structures is. In cardiac valves, bone can form within a dystrophic plaque so it is possible that even if this structure in the Gorilla was a dystrophic plaque, it could act as precursors to os cordis (Mohler et al. 2001).

Both structures in G3 and G11 stained similarly with alcian blue at pH 0.2, this stain was used primarily to identify cartilage and since neither structures stained positively and no chondrocytes were observed, the indication was that no cartilage was present. When exposed to Von Kossa stain both hyperdense structures stained positively for calcium. This was to be expected as both structures presented similarly to calcified dystrophic plaques or bone, both of which would stain positively when exposed to the Von kossa stain (Meloan & Puchtler, 1985). When this evidence from special stains is combined with morphological observations from H+E staining observations it was possible to confirm that the structure found in G11 was a calcified dystrophic plaque. However, the structure found in G3 could not be identified as either a plaque or a bone since its morphological appearance was similar to bone but no other evidence of bone was found.

In conclusion, when all factors are considered it is highly likely that the hyperdense structure found in Gorilla sample G11 was a dystrophic plaque due to its homogenous internal matrix observed by H+E staining. The structure did not stain strongly with alcian blue (to identify cartilage) nor did it present with any identifiable bone or cartilage cell types, or any other cell type, and so is highly unlikely to be cartilage or bone. Additionally, this structure stained positively for calcium presence, had no trabeculation during microCT analysis and merited no positive cells from immunohistochemistry staining.

The hyperdense structure found in G3 could not be as clearly defined. The structure also did not stain strongly with alcian blue, contained no identifiable cell types within the structure and stained positively for calcium. This indicated that the structure was also a dystrophic plaque. However, H+E staining did show that the structure looked morphologically similar to bone and contained some trabeculation like structure. The morphological appearance of the structure alone was not enough evidence to suggest the structure was bone but could suggest that with further investigation of Gorilla hearts bone tissue and subsequent os cordis may yet be discovered. This

alongside continued assessment of fibrosis levels in hearts and differing ages could merit similar results to those found in the chimpanzee (Moittie et al. 2020).

6. Final Discussion and Conclusions

The investigations in this study have merited the novel discovery of four ossa cordis in the nyala and have fully examined the giraffe os cordis for the first time using radiology, dissection and histology. Furthermore, using the same techniques, the analysis of 15 Gorilla and nine bonobo hearts merited the discovery of a hyperdense structure in two Gorilla hearts. One of these structures could be confirmed as a dystrophic plaque while the other could not be as clearly defined, is suspected to be either a dystrophic plaque or bone.

MicroCT scans showed trabeculation of the bone(s) found in the nyala and giraffe and displayed that the largest hyperdense structure found in the Gorilla, which would later be confirmed as a dystrophic plaque had a hyperdense shell and less dense interior. Histological techniques confirmed presence of bone in the nyala and giraffe, and was used to identify characteristics of hyperdense structures found in Gorilla hearts. The bone marrow of the nyala ossa cordis were made up of hematopoietic cells whereas the marrow in the giraffe os cordis was predominantly adipose tissue. Histology was also able to show a dense cortical layer around the dystrophic plaque found in the Gorilla. In addition, a bone-like morphology was observed in the other hyperdense tissue also found in a Gorilla heart (G3).

The discovery of os(sa) cordis in the giraffe and nyala in a single heart of both species. Although investigation of more hearts from each species is required, the discovery of os(sa) cordis or cartilago cordis in small sample sizes is frequent. Os(sa)/ cartilago cordis has been found in only one heart in an elephant, rhinoceros and a horse as well as now in the giraffe and nyala (Endo et al 2005; Erdogan et al. 2014; Matsuda et al. 2010; Perez et al. 2008). All of these species should be investigated for os(sa)/ cartilago cordis with a larger sample size.

The discovery of four ossa cordis in the nyala was entirely novel and has never been seen in any other species whereas, one os cordis has been seen in goats, deer, camels, chimpanzees, dogs, cats, a horse and otters as well as in the giraffe in this study (Mohammadpour & Arabi, 2007; Rumph, 1975; Ghonimi et al. 2014; Moittie et al. 2020; James & Drake, 1968; Liu et al. 1975; Matsuda et al. 2010; Ergerbacher et al. 2000; Pour, 2004; Frink & Merrick, 1974).

The OCD found in the nyala heart was directly comparable in shape to that of cattle (Figure. 3.2; Figure. 4.2). The bone was t-shaped with a major projection in its cranial third. Although the bone was a comparable shape to cattle, the size of the bone was considerably smaller (26mm in length compared to an average length in cattle of 42.5mm; Pour, 2004; James, 1965). The os cordis superior sinistrum in the nyala was similar in shape to OCD in goats but was more similar to sheep OCD in length (around 10-15mm; Frink & Merrick). The smaller two bones in the nyala heart, os cordis intermedius and inferior sinistrum were irregularly triangular in shape, similar to those found in the otter and were similar in size to os cordis in the chimpanzee or OCS in sheep (Ergerbacher et al. 2000; Moittie et al. 2020; Frink & Merrick, 1974). The single os cordis found in the giraffe was smaller than the OCD in the nyala but larger than the largest OCS in the nyala. It had a rectangular shape and was a similar size to OCD found in Iranian-breed sheep (Mohammadpour & Arabi, 2007). The size of the two hyperdense strucutres found in two Gorilla hearts were smaller than most os cordis, both of them measuring smaller than the average of any previously found ossa cordis at 2-3mm in length and less than 1mm in width and depth.

The two nyala bones, single giraffe bone and hyperdense structure in the Gorilla were found in the region of the major cardiac septa and shared similar positions to os(sa) cordis cattle, sheep and otters as well as cartilago cordis in hamsters (James, 1965; Frink & Merrick, 1974; Ergerbacher et al. 2000; Duran et al. 2004). The positions of the other two bones were less comparable to other species, the most cranial part of OCD in cattle and camels reside in this regions but only the white-tailed deer presents with a whole bone here (James, 1965; Ghonimi et al. 2014; Rumph, 1975). Regarding the largest bone found in the nyala heart, only one account of bone tissue in the right atria of sheep is comparable but the bone seen on these occasions were much smaller (Gopalakrishnan, 2007). The position of the dystrophic plaque found in a Gorilla aorta is not comparable to the positions of any other hyperdense structures encountered as part of this thesis.

The leading hypothesis toward the formation of os(sa) cordis in all species is EO, the development of bone from cartilage. Evidence of this theory acting in os(sa) cordis development has been seen in water buffalo, otters, camels, sheep and chimpanzees as well as supporting evidence in dogs and cattle (Daghash & Farghali, 2017; Ergerbacher et al. 2000; Ghonimi et al. 2014; Moittie et al. 2020; Gopalakrishnan, 2007; James, 1965; James & Drake, 1968). Investigations into os(sa) cordis discovered in the nyala and giraffe heart can add supporting evidence to this theory. Cartilage was present adjacent to the largest os cordis of the nyala and the giraffe os cordis and chondrocytes were observed invading into bone tissue displaying direct evidence of EO. EO requires constant involvement of type III collagen and following analysis of giraffe stained tissue it was observed that tissue surrounding bone had a much greater proportion of green (likely type III) fibers than tissue away from bone (84% compared to 58%). Observations seen in otters prompted the suggestion that os cordis formation by EO was related to high mechanical forces (Ergerbacher et al. 2000). Although the position of the bones observed in the nyala and giraffe were in locations of high

mechanical load, it was not possible to prove that high mechanical forces played a role in os(sa) cordis formation. In chimpanzees, it has been suggested that HO may play a role in os(sa) cordis development (Moittie et al. 2020). Additionally, observations made in the development of the rat os penis has shown that development of interstitial bones can occur by a combination of processes, in this case EO and IMO. It is therefore possible that os(sa) cordis develops by a combination of EO and HO/ IMO however, only evidence of EO was seen in these investigations.

The development of os(sa) cordis by EO requires an initial presence of cartilage in the heart. It has been suggested that cartilago cordis develops from NCC's in in hamsters, chinchillas, chickens, terrapins and quails (Duran et al. 2004; Warchulska et al. 2016; Lopez et al. 2001; Lopez et al. 2003; Lopez et al. 2000). This has also been suggested following observations of os(sa) cordis in camels and sheep (Ghonimi et al. 2014; Gopalakrishnan, 2007). However, cardiac fibrocytes can also be responsible for the formation of cartilage in the heart, via EMT (Von Gisse & Pu, 2012).

Due to the position of the os(sa) cordis found in the heart of the nyala and giraffe it was deduced that the function of the bones was likely to protect vital structures in the heart. This hypothesis was first suggested regarding os cordis in cattle but has since been suggested following discovery of os(sa) cordis in sheep and otters as well as supporting evidence from the discovery of cartilago cordis in the platypus. (James, 1965; Frink & Merrick, 1974; Ergerbacher et al. 2000; Davies, 1931). It is possible that os(sa) cordis may have more functions. The human cardiac for example, aids the coordination of cardiac contraction by allowing myocardial fibers to insert into it acting as an anchor against contraction (Trainini et al. 2020). It is possible that os(sa) cordis and cartilago cordis also perform this role and such has been suggested to occur in cattle and camels, where cardiac myocytes were found inserting into os cordis (James, 1965; Pour, 2004; Ghonimi et al. 2014). No cardiac myocytes were observed in the os(sa) cordis of the nyala or giraffe however, this does not rule out the possibility that they play a role in cardiac contraction. Observation of the hyperdense structures found in two Gorilla hearts did not merit the suggestion of their function but, it is plausible that due to a degree of CVD being found in the two hearts, that the hyperdense structures provide no function and are instead of pathological origin.

Histological investigations of the hearts of Gorillas, bonobos, a giraffe and a nyala in this thesis all showed abnormally high levels of adipocytes and erythrocytes within myocardial tissue. In addition, 'wavy' abnormal tissue was seen in all four investigated species. These observations alone do not suggest that the hearts were diseased, although all 24 hearts from the great apes did present with at least some level of fibrosis during an assessment by a veterinary pathologist. CVD has been strongly linked to the occurrence of os(sa) cordis (Moittie et al. 2020; James & Drake, 1968; Liu et al. 1975; Matsuda et al. 2010). It is thought that os(sa) cordis development occurs during CVD as a result of cardiac conditions caused by disease such as ischemia, abnormal tissue repair and high mechanical forces (Lehoczky-Mona & McCandles, 1964; Aljinovic et al. 2016; Stiener et al. 2007). Not only that

but, it was also suggested from a study on dogs with os cordis that the presence of os cordis can worsen that state of CVD by promoting further adverse cardiac conditions, such as ischemia (James & Drake, 1968).

Statistical analysis of the given fibrosis levels of Gorilla and bonobo hearts compared to their age merited no significant correlations between age and fibrosis of the hearts studied. However, this was expected as the hearts chosen in this study aimed to investigate hearts of many ages and differing levels of fibrosis so that if hyperdense tissues were found correlations could be identified between age, fibrosis and presence of hyperdense tissues. Only two Gorilla hearts with hyperdense tissues were found and these hearts belonged to fibrosis level two out of five and four out of five. Also, both were middle-aged compared to all hearts studied so, it was not possible to deduce a correlation between age or fibrosis level and occurrence of hyperdense tissues. Despite the lack of statistical findings in this study, it has been shown that os cordis is more likely to occur with a higher fibrosis level in chimapnzees (Moittie et al. 2020). Also, it has been shown in animals and humans that levels of fibrosis increases with age (Mukherjee & Sen, 1990; Song et al. 1999). Since fibrosis is thought to increase with age and os cordis occurrence has been shown to be related to fibrosis it can be deduced that os cordis occurrence is more likely to occur with age. This has been seen in water buffalo, elephants, dogs, and otters (Daghash & Farghali, 2017; Endo et al. 2005; James & Drake, 1968; Ergerbacher et al. 2000). This contrasts to what has been shown regarding cartilago cordis where in hamsters, during old age cartilago cordis occurs less frequently (Duran et al. 2004).

A theme which has reoccurred throughout this thesis is the theory that os cordis development is predisposed to genetic trends among species. For example, the *Atriodactyla* order has many more species, including two which were investigated in this study, with os(sa) cordis present compared to other phylogenetic orders. The same such trends were not observed with regards to cartilago cordis. To confirm that genetics plays a role in species having or not having os(sa) cordis, more evolutionary links must be investigated and analysed. At present the mere observation that many species have os cordis in one phylogenetic group compared to others does not prove there is an evolutionary/ genetic link to the occurrence of os(sa) cordis.

Across most species where an os cordis has been identified, os(sa) cordis rarely occur in all of the individuals studied. In cases such as the chimpanzee, otter, goat, cat and elephant os cordis was present in less than 50% of the hearts studied (Moittie et al 2020; Ergerbacher et al. 2000; Mohammadpour & Arabi, 2007; Liu et al. 1975; Endo et al. 2005). In all of the studies to date, including the present one, it is possible that hyperdense structures and even bone have been missed. Hence, novel discoveries of os(sa) cordis could have been missed at a species level and at an individual level.

A deeper understanding of the factors involved in the formation of hyperdense cardiac structures could provide more precise methods of finding and examining hyperdense structures. This thesis has shown that computerised analysis of PSR stains alongside an assessment of fibrosis levels can be effective in finding changes or differences in collagen proportions in heart samples. However, simply finding a higher proportion of type I collagen fibers and/or high fibrosis levels is not enough to indicate or predict that os cordis formation will occur in a given species or individual, nor can it predict the formation of any other hyperdense tissues.

PSR analysis alongside an assessment of fibrosis levels should be carried out on a larger number of species known to develop os cordis across varying ages. Undertaking this could allow us to determine a threshold proportion of type I collagen (or red fibers when stained using PSR) and fibrosis level which would more definitely suggest os cordis formation is going to/ is occurring.

Applying thresholds to the likelihood of os(sa) cordis forming has not only a research application, but also could be applied to clinical settings. In cases such as the dog, formation of hyperdense tissue has been known to increase the severity of disease and therefore worsen prognosis (James & Drake, 1968). Having a threshold of type I collagen/ fibrosis (or another factor) alongside age and other variables could allow a clinician to judge the 'threat-level' of hyperdense tissues forming. Therefore, by taking a sample of heart tissue and assessing its fibrosis level, type I collagen proportions and other key features, clinicians from both veterinary and human medicine could better predict prognosis in cases of CVD, namely IMF.

In all this thesis has discovered four ossa cordis in the nyala which is entirely novel regarding its presence and number. Additionally, a proper investigation of the giraffe os cordis has been completed giving more details on the size, shape, position and morphology of the bone, which has not previously been noted. Perhaps most significantly this study has highlighted the significant gaps in scientific knowledge surrounding os cordis. This thesis has shown that there is much potential in the discoveries that can be made, not only regarding os cordis in more species, but also to improve scientific knowledge of the bone as a whole. This knowledge can have far-reaching implications to improve not only anatomical but clinical understandings surrounding the heart and CVD.

References

AGUIAR, A. M. D., KULIGOVSKI, C., COSTA, M., STIMAMIGLIO, M., REBELATTO, C.,
SENEGAGLIA, A., BROFMAN, P. R. S., DALLAGIOVANNA, B., GOLDENBERG, S. & CORREA, A. 2011. Alkaline phosphatase-positive cells isolated from human hearts have mesenchymal stem cell characteristics. Stem Cell Discovery, 1, 71-80.

ALJINOVIC, J., VUKOJEVIC, K., SARAGA-BABIC, M., GUIC, M., KOSTA, V., POLJINCANIN, A. &
GRKOVIC, I. 2016. A Bone in the Rat's Heart. 3 ed.: J Biomed.

ANDERSON, K. R., SUTTON, M. G. & LIE, J. T. 1979. Histopathological types of cardiac fibrosis in myocardial disease. J Pathol, 128, 79-85.

ANDERSON, R.H., YANNI, J., BOYETT, M.R., CHANDLER, N.J., DOBRZYNSKI, H. 2009. The anatomy of the cardiac conduction system. Clin Anat, 22(1), 99-113

BAJUSZ, E. 1969. Dystrophic calcification of myocardium as conditioning factor in genesis of congestive heart failure. An experimental study. Am Heart J, 78, 202-10.

BARASCH, E., GOTTDIENER, J. S., LARSEN, E. K., CHAVES, P. H., NEWMAN, A. B. & MANOLIO, T. A. 2006. Clinical significance of calcification of the fibrous skeleton of the heart and aortosclerosis in community dwelling elderly. The Cardiovascular Health Study (CHS). Am Heart J, 151, 39-47.

BERENDSEN, A. D. & OLSEN, B. R. 2015. Bone development. Bone, 80, 14-18.

BISHOP, J. E. & LINDAHL, G. 1999. Regulation of cardiovascular collagen synthesis by mechanical load. Cardiovasc Res, 42, 27-44.

BRAZ, J. K., FREITAS, M. L., MAGALHÃES, M. S., OLIVEIRA, M. F., COSTA, M. S., RESENDE, N.
S., CLEBIS, N. K., SILVA, N. B. & MOURA, C. E. 2016. Histology and Immunohistochemistry of the Cardiac Ventricular Structure in the Green Turtle (Chelonia mydas). Anat Histol Embryol, 45, 277-84.

CHEN, L., QIU, Q., JIANG, Y., WANG, K., LIN, Z., LI, Z., BIBI, F., YANG, Y., WANG, J., NIE, W.,
SU, W., LIU, G., LI, Q., FU, W., PAN, X., LIU, C., YANG, J., ZHANG, C., YIN, Y., WANG, Y., ZHAO, Y., WANG, Z., QIN, Y., LIU, W., WANG, B., REN, Y., ZHANG, R., ZENG, Y., DA FONSECA, R. R., WEI, B., LI, R., WAN, W., ZHAO, R., ZHU, W., DUAN, S., GAO, Y., ZHANG, Y. E., CHEN, C., HVILSOM, C., EPPS, C. W., CHEMNICK, L. G., DONG, Y., MIRARAB, S., SIEGISMUND, H. R., RYDER, O. A., GILBERT, M. T. P.,

LEWIN, H. A., ZHANG, G., HELLER, R. & WANG, W. 2019. Large-scale ruminant genome sequencing provides insights into their evolution and distinct traits. Science, 364.

CISZEK, D. 1999. Tragelaphus angasii (On-line), Animal Diversity Web. Accessed August 22, 2021 at https://animaldiversity.org/accounts/Tragelaphus_angasii/

DAGHASH, S. & FARGHALI, H. 2017. The cardiac skeleton of the Egyptian Water buffalo (Bubalus bubalis). Int. J. Adv. Res. Biol. Sci, 4, 1-13.

DAVIES, F. 1931. THE CONDUCTING SYSTEM OF THE MONOTREME HEART. Anatomy Department, King's College, London.

DE ALMEIDA, M., SANCHEZ-QUINTANA, D., DAVIS, N., CHARLES, F., CHIKWETO, A., SYLVESTER, W., LOUKAS, M. & ANDERSON, R. 2019. The ox atrioventricular conduction axis compared to human in relation to the original investigation of sunao tawara. 3 ed.: Clinical Anatomy.

DESSAU, W., VON DER MARK, H., VON DER MARK, K. & FISCHER, S. 1980. Changes in the patterns of collagens and fibronectin during limb-bud chondrogenesis. J Embryol Exp Morphol, 57, 51-60.

DUPUY, G. 2011. The deer's cross. Les Cahiers Cynegetiques Du Naturaliste.

DURAN, A. C., LOPEZ, D., GUERRERO, A., MENDOZA, A., ARQUE, J. M. & SANS-COMA, V. 2004. Formation of cartilaginous foci in the central fibrous body of the heart in Syrian hamsters (Mesocricetus auratus). J Anat, 205, 219-27.

EGERBACHER, M., WEBER, H. & HAUER, S. 2000. Bones in the heart skeleton of the otter (Lutra lutra). The Journal of Anatomy, 196, 485-491.

ENDO, H., SAKAI, T., ITOU, T., KOIE, H. & KIMURA, J. 2005. Macroscopic observation and CT examination of the heart ventricular walls in the Asian elephant. Mammal Study.

ERDOĞAN, S., LIMA, M. & PÉREZ, W. 2014. Inner ventricular structures and valves of the heart in white rhinoceros (Ceratotherium simum). Anat Sci Int, 89, 46-52.

FALK, E. 2006. Pathogenesis of atherosclerosis. J Am Coll Cardiol, 47, C7-12.

FERRIS, J. A. & AHERNE, W. A. 1971. Cartilage in relation to the conducting tissue of the heart in sudden death. Lancet, 1, 64-6.

FRINK, R. J. & MERRICK, B. 1974. The sheep heart: coronary and conduction system anatomy with special reference to the presence of an os cordis. Anat Rec, 179, 189-200.

GADE, T. P., MOTLEY, M. W., BEATTIE, B. J., BHAKTA, R., BOSKEY, A. L., KOUTCHER, J. A. & MAYER-KUCKUK, P. 2011. Imaging of alkaline phosphatase activity in bone tissue. PLoS One, 6, e22608.

GHONIMI, W. A., BALAH, A., BAREEDY, M. H. & ABUEL-ATTA, A. A. 2014. Os cordis of the mature dromedary camel heart (Camelus dromedaries) with special emphasis to the cartilago cordis.: Journal of Advanced Veterinary and Animal Research.

GOPALAKRISHNAN, G., BLEVINS, W. E. & VAN ALSTINE, W. G. 2007. Osteocartilaginous metaplasia in the right atrial myocardium of healthy adult sheep. J Vet Diagn Invest, 19, 518-24.

GÓMEZ-TORRES, F., BALLESTEROS-ACUÑA, L. & RUÍZ-SAURI, A. 2021. Morphological variations of the conduction system in the atrioventricular zone and its clinical relationship in different species. Anat Sci Int, 96, 212-220.

HABERMEHL, K. H. & SCHMACK, K. H. 1986. [The topography of the heart valves in horses, cattle and dogs]. Anat Histol Embryol, 15, 240-8.

HANSEN, J. & DR, L. 2005. Netter's Clinical Anatomy, Elsevier.

HEARTS CENTRAL. 2010. Anatomy Continued (On-line), Accessed August 28, 2021 at https://heartscentral.wordpress.com/2010/05/05/anatomy-continued/

ICARDO, J. M. & COLVEE, E. 1995. Atrioventricular valves of the mouse: II. Light and transmission electron microscopy. Anat Rec, 241, 391-400.

JAMES, T. N. 1965. Anatomy of the sinus node, AV node and os cordis of the beef heart. The Anatomical Record, 153, 361-371.

JAMES, T. N. & DRAKE, E. H. 1968. Sudden death in Doberman pinschers. Ann Intern Med, 68, 821-9.

JAMES, T. N., KAWAMURA, K., MEIJLER, F. L., YAMAMOTO, S., TERASAKI, F. & HAYASHI, T. 1995. Anatomy of the sinus node, AV node, and His bundle of the heart of the sperm whale (Physeter macrocephalus), with a note on the absence of an os cordis. The Anatomical Record, 242, 355-373.

JURADO, S., DA SILVA, R. & MORCELI, V. 2006. Morphology of the atrioventricular junction in Iguana iguana (Reptilia-Iguanidae). 3 ed.: Brazilian Journal of Veterinary Research and Animal Science.

KAPLAN, F. S., GLASER, D. L., HEBELA, N. & SHORE, E. M. 2004. Heterotopic ossification. J Am Acad Orthop Surg, 12, 116-25.

KUMAR, G. J. & KIERNAN, J. A. 2010. Educational Guide, Special Stains and H & E. Dako North America, 80-85.

LAMMEY, M. L., BASKIN, G. B., GIGLIOTTI, A. P., LEE, D. R., ELY, J. J. & SLEEPER, M. M. 2008. Interstitial myocardial fibrosis in a captive chimpanzee (Pan troglodytes) population. Comp Med, 58, 389-94.

LATTOUF, R., YOUNES, R., LUTOMSKU, D., NAAMAN, N., GODEAU, G., SENNI, K. & CHANGOTADE, S. 2014. Picrosirius Red Staining: A useful Tool to Appraise Collagen Networks in Normal and Pathological Tissues. Journal of Histochemistry & Cytochemistry, 62(10), 751-758.

LEHOCZKY-MONA, J. & MCCANDLES, E. 1964. Ischemic induction of chrondrogenesis in myocardium. Chicago: Archives of Pathology & Laboratory Medicine.

LIU, S., TILLEY, L. & TASHJIAN, R. 1975. Lesions of the conduction system in the cat with cardiomyopathy. Recent Advances in Studies on Cardiac Structure and Metabolism.

LOPEZ, D., DURAN, A. C. & SANS-COMA, V. 2000. Formation of cartilage in cardiac semilunar valves of chick and quail. Ann Anat, 182, 349-59.

LOWENSTINE, L. J., MCMANAMON, R. & TERIO, K. A. 2016. Comparative Pathology of Aging Great Apes: bonobos, Chimpanzees, Gorillas, and Orangutans. Vet Pathol, 53, 250-76.

LÓPEZ, D., DURÁN, A. C., DE ANDRÉS, A. V., GUERRERO, A., BLASCO, M. & SANS-COMA, V. 2003. Formation of cartilage in the heart of the Spanish terrapin, Mauremys leprosa (Reptilia, Chelonia). J Morphol, 258, 97-105.

LÓPEZ, D., FERNÁNDEZ, M. C., DURÁN, A. C. & SANS-COMA, V. 2001. Cartilage in pulmonary valves of Syrian hamsters. Ann Anat, 183, 383-8.

MAISANO, S. 2006. Giraffa camelopardalis (On-line), Animal Diversity Web. Accessed August 22, 2021 at https://animaldiversity.org/accounts/Giraffa_camelopardalis/

MATSUDA, K., TABATA, S., KAWAMURA, Y., KUROSAWA, T., YOSHIE, N. & TANIYAMA, H. 2010. Ectopic ossification with haematopoietic bone marrow in the heart valves of a crossbreed heavy horse. 2-3 ed.: Journal of Comparative pathology.

MEYERS, C., LISIECKI, J., MILLER, S., LEVIN, A., FAYAD, L., DING, C., SONO, T., MCCARTHY, E., LEVI, B. & JAMES, A. W. 2019. Heterotopic Ossification: A Comprehensive Review. JBMR Plus, 3, e10172.

MOHAMMADPOUR, A. & ARABI, M. 2007. Morphological study of the heart and Os cordis in sheep and goat. 3 ed.: The Indian veterinary journal.

MOHLER, E. R., GANNON, F., REYNOLDS, C., ZIMMERMAN, R., KEANE, M. G. & KAPLAN, F. S. 2001. Bone formation and inflammation in cardiac valves. Circulation, 103, 1522-8.

MOITTIÉ, S., BAIKER, K., STRONG, V., COUSINS, E., WHITE, K., LIPTOVSZKY, M., REDROBE, S., ALIBHAI, A., STURROCK, C. J. & RUTLAND, C. S. 2020. Discovery of os cordis in the cardiac skeleton of chimpanzees (Pan troglodytes). Sci Rep, 10, 9417.

MUKHERJEE, D. & SEN, S. 1990. Collagen phenotypes during development and regression of myocardial hypertrophy in spontaneously hypertensive rats. Circ Res, 67, 1474-80.

MURAKAMI, R. 1986. Development of the os penis in genital tubercles cultured beneath the renal capsule of adult rats. J Anat, 149, 11-20.

NABIPOUR, A. & SHAHABODINI, M. 2007. Histological study of the AVN and bundle in the heart of ovine fetus. 1 ed.: Iranian Journal of Veterinary Research.

NASOORI, A. 2020. Formation, structure, and function of extra-skeletal bones in mammals. Biol Rev Camb Philos Soc, 95, 986-1019.

PEREZ, W., LLMA, M. & PEDRANA, G. 2008. Heart anatomy of Giraffa camelopardalis rothschildi: A case report. 3 ed.: Veterinami Medicina.

POUR, A. 2004. Comparative morphometry of the heart in Holstein and a native Iranian cow breeds wth emphasis on the OS cordis. Indian Veterinary Journal, 81, 806-809.

RANGANATHAN, K., LODER, S., AGARWAL, S., WONG, V. W., WONG, V. C., FORSBERG, J., DAVIS, T. A., WANG, S., JAMES, A. W. & LEVI, B. 2015. Heterotopic Ossification: Basic-Science Principles and Clinical Correlates. J Bone Joint Surg Am, 97, 1101-11.

ROSS, M. & PAWLINA, W. 2016. Histology : a text and atlas : with correlated cell and molecular biology. 7 ed.

RUMPH, P. 1975. Osteology of the White-Tailed Deer. Auburn University.

RUTLAND, C. S., COCKCROFT, J. M., LOTHION-ROY, J., HARRIS, A. E., JEYPALA, J. N., SIMPSON, S., ALIBHAI, A., BAILEY, C., BALLARD-REISCH, A. C., RIZVANOV, A. A., DUNNING, M. D., DE BROT, S., & MONGAN, N. P. 2021. Immunohistochemical Characterisation of GLUT1, MMP3and NRF2 in Oseateosarcoma. Frontiers in veterinary science, 8.

ROTH, J. 2004. Bubalus bubalis (On-line), Animal Diversity Web. Accessed August 22, 2021 at https://animaldiversity.org/accounts/Bubalus_bubalis/

SASASN, J., PIYUSH, P., SINGH, A., JOHN, M. & MALIK, M. 2015. Biometry of the heart of fowl. Indian Journal of Animal Research.

SCHMACK, K. 1974. Die Ventilebene des Herzens bei Pferd, Rind und Hund.: Veterinary Medicine, University of Giesson.

SHACKLEY, B. S., NGUYEN, T. P., SHIVKUMAR, K., FINN, P. J. & FISHBEIN, M. C. 2011. Idiopathic massive myocardial calcification: a case report and review of the literature. Cardiovasc Pathol, 20, e79-83.

SINGHA, B. 2018. Dyce, Sack and Wensing's textbook of veterinary anatomy. Elsevier Health Sciences.

SJAASTAD, O., SAND, O. & HOVE, K. 2010. Physiology of Domestic Animals. 2 ed.: Scandinavian Veterinay Press.

SN, M. & H, P. 1985. Chemical mechanisms of staining methods: von Kossa's technique: what von Kossa really wrote and a modified reaction for selective demonstartion of inorganic phosphates. 1 ed.: Journal of Hostotechnology.

SOLIMAN, M. K. Functional anatomical adaptations of dromedary (Camelus Dromedaries) and ecological evolutionary impacts in KSA. International Conference on Plant, Marine and
Environmental Sciences (PMES-2015) Kuala Lumpur (Malaysia), 2015.

SONG, Y., YAO, Q., ZHU, J., LUO, B. & LIANG, S. 1999. Age-related variation in the interstitial tissues of the cardiac conduction system; and autopsy study of 230 Han Chinese. Forensic Sci Int, 104, 133-42.

STEINER, I., KASPAROVA, P., KOHOUT, A. & DOMINIK, J. 2007. Bone formation in cardiac valves: a histopathological study of 128 cases. Virchows Arch.

STRONG, V., MOITTIÉ, S., SHEPPARD, M. N., LIPTOVSZKY, M., WHITE, K., REDROBE, S., COBB, M. & BAIKER, K. 2020. Idiopathic Myocardial Fibrosis in Captive Chimpanzees (Vet Pathol, 57, 183-191.

SUMIDA, H., AKIMOTO, N. & NAKAMURA, H. 1989. Distribution of the neural crest cells in the heart of birds: a three dimensional analysis. Anat Embryol (Berl), 180, 29-35.

TIRZIU, D., GIORDANO, F. J. & SIMONS, M. 2010. Cell communications in the heart. Circulation, 122, 928-37.

TRAININI, J., LOWENSTEIN, J., BERAUDO, M., WERNICKIE, M., TRAININI, A., LLABATA, V. & CARRERAS, C. 2020. Myocardial torsion and cardiac fulcrum. Morphologie.

VON GISE, A. & PU, W. T. 2012. Endocardial and epicardial epithelial to mesenchymal transitions in heart development and disease. Circ Res, 110, 1628-45.

WARCHULSKA, K., BARSZCZ, K., GARNCARZ, M. & DZIERZANOWSKA-GORYN, D. 2016. Presence of cartilagenous foci in the left atrioventricular opening of the chinchilla's heart. 4 ed.: Medycyna Weterynaryjna.

WU, C. Y., MARTEL, J. & YOUNG, J. D. 2020. Ectopic calcification and formation of mineralo-organic particles in arteries of diabetic subjects. Sci Rep, 10, 8545.

WULF, M., BOSSE, A., WIETHEGE, T., VOSS, B. & MÜLLER, K. M. 1994. Localization of collagen types I, II, and III mRNAs in human heterotopic ossification by non-radioactive in situ hybridization. Pathol Res Pract, 190, 25-32.

YANIV, Y., TSUTSUI, K. & LAKATTA, E. G. 2015. Potential effects of intrinsic heart pacemaker cell mechanisms on dysrhythmic cardiac action potential firing. Front Physiol, 6, 47.

YOUNG, B. A. 1994. Cartilago cordis in serpents. Anat Rec, 240, 243-7.

Appendix. 1. MicroCT Scans of Seven Gorilla Hearts
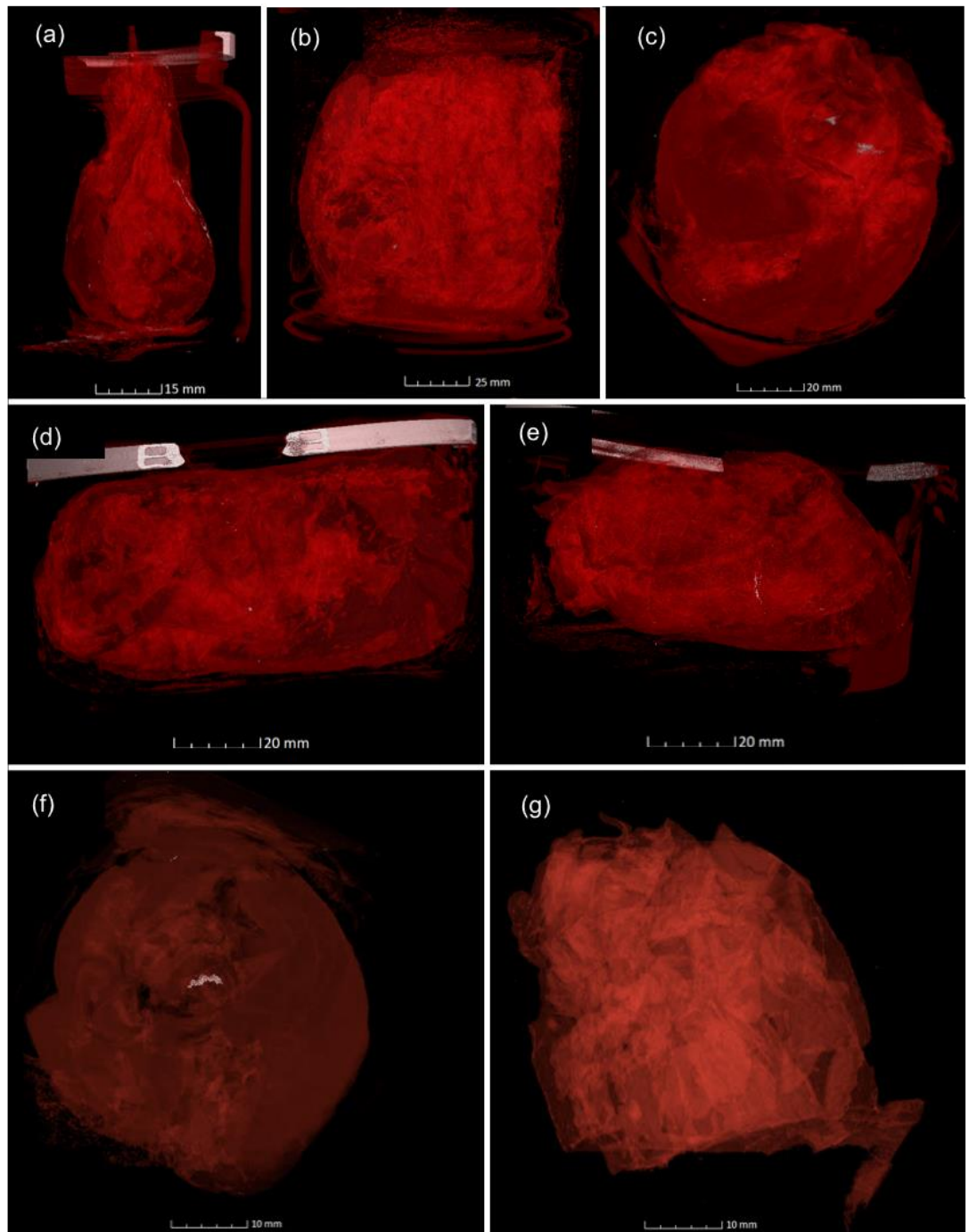
Figure. Appendix. 1. MicroCT scans of seven Gorilla hearts. (a) G7. (b) G1. (c) G15. (d) G17. (e) G4. (f) G10. (g) G9. Scale bars represent 15mm (a), 25mm (b), 120mm (c-e) and 10mm (f+g).

Appendix. 2. Table of regions of interest taken from Gorilla and bonobo hearts following microCT

Heart	Location of ROI	Number of samples taken from ROI	Evidence of HD tissue found?
B2	Aorta	1	No
	Atrial Wall	2	No
B3	Right AV Valve	1	No
	Right Atrial Wall	1	No
B4	Atrial Wall	2	No
	Left Auricle	1	No
B6	Atrial Wall near AV Valve	1	No
B9	Atrial Wall near AV Valve	3	No
G1	Atrial Wall	2	No
G3	Atrial Wall	1	No
	Interatrial Septa	1	**Yes**
G4	Atrial Wall	2	No
G7	Atrial Wall	2	No
G8	Interatrial Septa	1	No
	Aorta	1	No
G10	Left AV Valve	1	No
G11	Aorta	3	**Yes**
G17	Base of Aorta	2	No
G15	Aorta	2	No
	Interatrial Septa	2	No

Table. Appendix. 2. A table showing all 20 regions of interest identified from microCT, the locations they were found in and whether hyperdense (HD) tissue was found in them after histology.

Appendix. 3. Chart of varying collagen percentages in different Gorilla and bonobo heart samples.
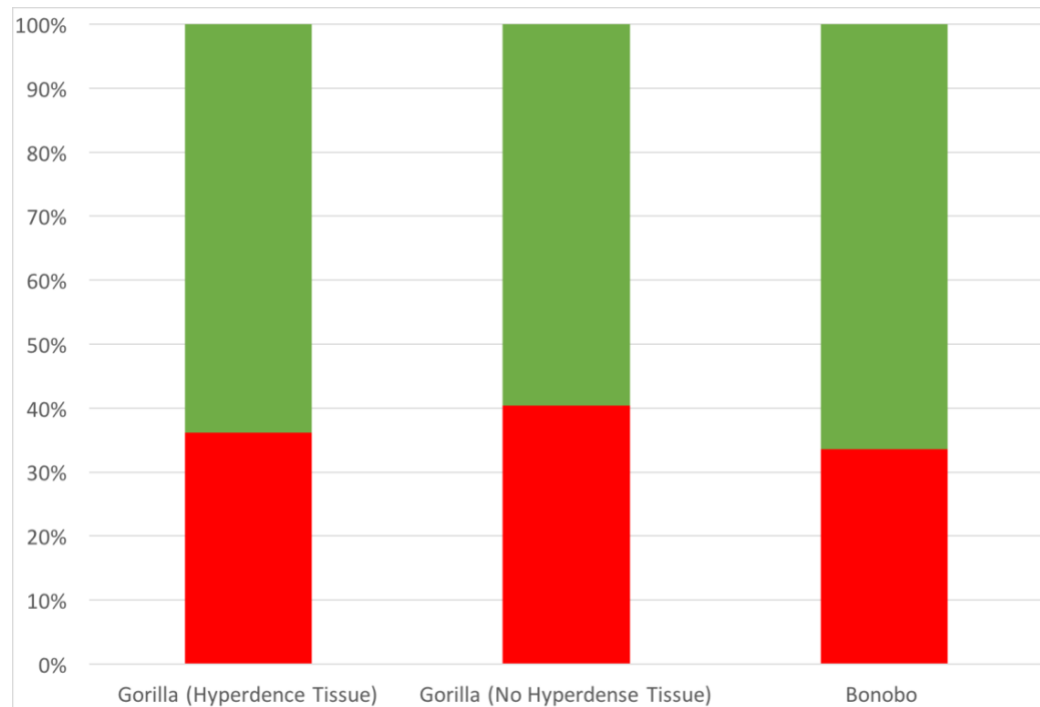
% Collagen	Gorilla (HD Tissue)	Gorilla (No HD Tissue)	bonobo
Green Fibers (likely type III)	64%	60%	66%
Red Fibers (likely type I)	36%	40%	34%

Figure. Appendix. 3. A 100% stacked bar chart showing varying ratios of collagen fibers (green: red) bellow a table outlining the same ratios as a percentage in bonobo and Gorilla hearts. Green represents fine fibers (likely type III) and red represents thick fibers (likely type I). Gorilla heart samples were divided into those with, and those without, hyperdense tissue prior to analysis.

Appendix. 4. Samples taken from each heart studied and their original locations.

Heart Species, Number	Sample Name(s)	Location(s)
Gorilla 1	G1x, G1y, G1A, G1B	Left atrial wall (x&y), interatrial septum (A), aortic wall (B)
Gorilla 2	G2A, G2B	Interatrial septum (A), left atrial wall (B)
Gorilla 3	G3x, G3y	Left atrial wall (x), interatrial septum near base of the aorta (y)
Gorilla 4	G4x, G4y, G4A, G4B	Left atrial wal (x&y), interatrial septum (A), aortic valve (B)
Gorilla 6	G6A, G6B	Left atrial wall (A), interatrial septum (B)
Gorilla 7	G7x, G7y	Left atrial wal (x&y)
Gorilla 8	G8x, G8y	Interatrial septum (x), aortic wall (y)
Gorilla 9	G9A, G9B	Myocardium near base of the aorta (A), interatrial septum (B)
Gorilla 10	G10x, G10A, G10B, G10C	Left atrioventricular valve (x), aortic valve (A), interatrial septum (B), aortic wall (C)
Gorilla 11	G11Dx, G11Cx, G11Cy	Aortic wall (Dx, Cx, Cy)
Gorilla 12	G12A, G12B	Interatrial septum (A), aortic wall (B)
Gorilla 13	G13A	Left atrial wall (A)
Gorilla 15	G15x, G15y, G15w, G15z	Aortic wall (x&y), interatrial septum (w&z)
Gorilla 16	G16A, G16B	Left atrial wall (A), myocardium near base of the aorta (B)
Gorilla 17	G17x, G17y	Myocardium near base of the aorta (x&y)
bonobo 1	B1A, B1B, B1C, B1D	Left atrioventricular valve (A), right auricle (B), left atrial wall (C), right atrial wall (D)
bonobo 2	B2x, B2y, B2z, B2A	Major cardiac vessel (x), left atrial wall (y&z), left atrioventricular valve (A)
bonobo 3	B3x, B3y, B3A	Right atrioventricular valve (x), right atrial wall (y&A)
bonobo 4	B4x, B4y, B4z	Left atrial wall (x&y), left auricle (z)
bonobo 5	B5A, B5B, B5C	Left atrial wall (A), aortic wall (B), right atrioventricular valve (C)
bonobo 6	B6x, B6A, B6B	Left atrial wall (x), aortic wall (A), branch of the aorta (B)
bonobo 7	B7A	Left atrial wall (A)
bonobo 8	B8A	Aortic valve (A)
bonobo 9	B9x, B9y, B9z, B9a,	Aortic valve (x,y&z), aortic wall

	B9<u>b</u>	(<u>a</u>&<u>b</u>)
Giraffe	Gfa, Gfb, Gfc, Gfd, Gfe	Tissue surrounding dense structure in interatrial septum (a), dense structure in interatrial septum (b,c&d), second dense structure in different location of major cardiac septa (e)
Nyala	Ny1, Ny2, Ny3, Ny4, Ny5, Ny6, Ny7	Major cardiac septa (1&2), atrioventricular valve (3&4), right atrial wall (5), myocardium at base of the aorta (6&7)

Table. Appendix. 4. A list of all hearts investigated in this thesis, all samples taken from each heart and the location of those samples. (x, y, z & w) represent regions of interest in Gorilla & bonobo hearts. (A, B, C, D) represent representative samples from regions of interest in Gorilla & bonobo hearts. Giraffe (Gf) and nyala (Ny) samples are named by letters and numbers respectively and all samples were regions of interest.

Appendix. 5. List of Papers included in Section 3. Comprehensive Review of Os cordis and Cartilago Cordis

Reference	Summary	Location(s) in Text
Pour, 2004	An investigation of os cordis in two breeds of cattle (Holstien & Iranian)	3.2.2, 3.2.10, 3.4, 3.6, Table 3.3
James, 1965	Anatomy of os cordis in the beef heart	3.2.2, Table 3.1, 3.3, 3.4
Schmack, 1974	Noted cartilage development in a 5-year-old horse heart	3.2.2, 3.2.7, 3.6, 3.7
Habermehl & Schmack, 1986	Noted further evidence of cartilage in the horse heart	3.2.2, 3.7
Daghash & Farghali, 2017	Discovery of os cordis in the water buffalo	3.2.2, Table 3.2, 3.3, 3.4, 3.5, 3.6, Table 3.3
Mohammadpour & Arabi, 2007	An investigation of os cordis in sheep and goats	3.2.3, Table 3.2, 3.2.10, Table 3.3
Gopalakrishnan, 2007	Osteocartilagenous structures found in sheep right atria	3.2.3, 3.2.10, 3.3, 3.5
Frink & Merrick, 1974	Investigation of os cordis in sheep	3.2.3, Table 3.2, 3.2.10, 3.3, 3.4, 3.6, Table 3.3
Rumph, 1975	Discovery of os cordis in the white-tailed deer	3.2.3, Table 3.2, Table 3.3
Dupuy, 2011	The anatomy of os cordis in deer, found as a result of hunting	3.3.3, Table 3.2, 3.3, 3.4, 3.6, Table 3.3
Ghonimi et al. 2014	Investigation of os cordis in the dromedary camel	3.2.4, Table 3.2, 3.3, 3.4, 3.6, Table 3.3
Moittie et al. 2020	Novel discovery of os cordis in the chimpanzee	3.2.5, 3.2.7, Table 3.2, 3.3, 3.4, 3.5, 3.6, Table 3.3
James & Drake, 1968	Noted presence of os cordis in dogs after investigation of sudden death in Doberman pinschers	3.2.6, 3.2.7, Table 3.2, 3.3, 3.4, 3.5, 3.6, Table 3.3
Liu et al. 1975	Bone discovered in the hearts of cats with cardiomyopathy	3.2.6, 3.2.7, Table 3.2, 3.3, 3.4, 3.5, 3.6, Table 3.3
Matsuda et al. 2010	Bone developments in horses heart valves	3.2.7, Table 3.2, 3.3, 3.4, 3.5, 3.6, Table 3.3
Ergerbacher et al. 2000	The discovery of bone in the otter heart	3.2.8, Table 3.2, 3.3, 3.4, 3.6, Table 3.3, 3.9
Endo et al 2005	Investigation of the elephant heart noted presence of bone	3.2.9, Table 3.2, Table 3.3
Reference	**Summary**	**Location(s) in Text**

Perez et al 2008	Noted the presence of a single os cordis in the giraffe	3.2.9, Table 3.2, Table 3.3
Duran et al 2004	Discovery of cartilaginous foci in the Syrian hamster	3.3, 3.7, Table 3.4, 3.8, 3.9
Lopez et al. 2001	Cartilage found in the pulmonary valves of Syrian hamsters	3.3, 3.7, Table 3.4, 3.8, 3.9
Von Gisse & Pu, 2012	Investigated epitheial to mesenchymal transition during heart disease	3.3, 3.5
Nasoori, 2020	Outlines the formation of extra-skeletal bones	3.3
Bishop & Lindhal, 1999	Investigates the effect of mechanical forces on heart structure	3.3, 3.4
Sumida et al. 1989	Investigates the role of neural crest cell with reference to the heart	3.3, 3.5, 3.8
Murakimi et al. 1986	Investigates the formation of os penis in rats	3.3
James et al. 1995	Notes the absence of os cordis in sperm whales	3.4, 3.5
Trainini et al. 2020	Investigates the human cardiac fulcrum	3.4, 3.9
De Almeida et al. 2019	Compares ox and human atrioventricular conduction axis	3.4
Soliman, 2015	Notes the os cordis in the camel heart	3.4
Barasch et al. 2006	Investigates increasing calcification of heart tissue with age in humans	3.4
Hearts Central, 2010	A diagram of the conduction system of the heart	Figure 3.3
Aljinovic et al. 2016	Investigates a bone in the rat heart	3.5
Lehoczky-Mona & McCandles, 1964	Investigates the formation of cartilage in the presence of ischemia	3.5
Ferris & Aherne, 1971	Investigates the impact of cartilage in the heart during sudden death	3.5
Steiner et al 2007	A study of 128 cases of bone formation in cardiac valves	3.5
Gomez-Torres et al. 2021	A study of the conduction system in dogs, pigs and horses	3.5, 3.7
Nabipour & Shahabidoni, 2007	Investigation of the AVN in the hearts of sheep fetus'	3.6, Table 3.3
Warchulska et al 2016	Discovery of cartilage in the chinchilla heart	3.7, Table 3.4, 3.8, 3.9
Reference	**Summary**	**Location(s) in Text**
Lopez et al. 2003	Discovery of cartilage in the terrapin heart	3.7, Table 3.4, 3.8, 3.9

Lopez et al. 2000	Discovery of cartilage in the hearts of chickens and quails	3.7, Table 3.4, 3.8, 3.9
Jurado et al. 2006	Notes the presense of cartilage in the iguana	3.7
Braz et al. 2015	Discovery of cartilage in the heart of green sea turtles	3.7, 3.9
Sasasn et al. 2015	Noted the presence of cartilage in the aortic ring of fowl	3.7, 3.9
Erdogan et al. 2014	Discovery of cartilage in the heart of rhinoceros	3.7, Table 3.4
Davies, 1931	Discovery of cartilage in the AVN of platypus	3.7, 3.9
Icardo & Colvee, 1995	Studied the atrioventricular valves of mice	3.7
Young, 1994	Discovered cartilago cordis in snakes	3.7, Table 3.4, 3.9

Appendix. 6. Credits Earned During Course of the MRes

Name	Date Completed	Credits Earned
Nottingham Advantage Award – Art and Anatomy	17-Aug-20	10
Nottingham Advantage Award – Effective Volunteering	01-Oct-20	10
Nottingham Advantage Award – Career Skills for Vets	17-Mar-21	10
Anatomical Society Conference (1 day)	15-Oct-20	2
Introduction to statistics with SPSS	25-Nov-20	2
INSpire Studentship Conference (1 day)	28-Nov-21	2
Anatomical Society Conference (3 days)	08-Jan-21	6
Postgraduate Symposium (Presented & Chaired, 2 days)	02-Jun-21	7
EAVA Conference (Presented, 3 days)	30-Jun-21	9
Undergraduate Teaching (1hour Meeting)	18-Dec-20	1
Undergraduate Teaching (5hour Lab Teaching)	22-Apr-21	5
Undergraduate and postgraduate Teaching (4hour Microscope/image analysis Teaching)	27-Apr-21	4
Total		68